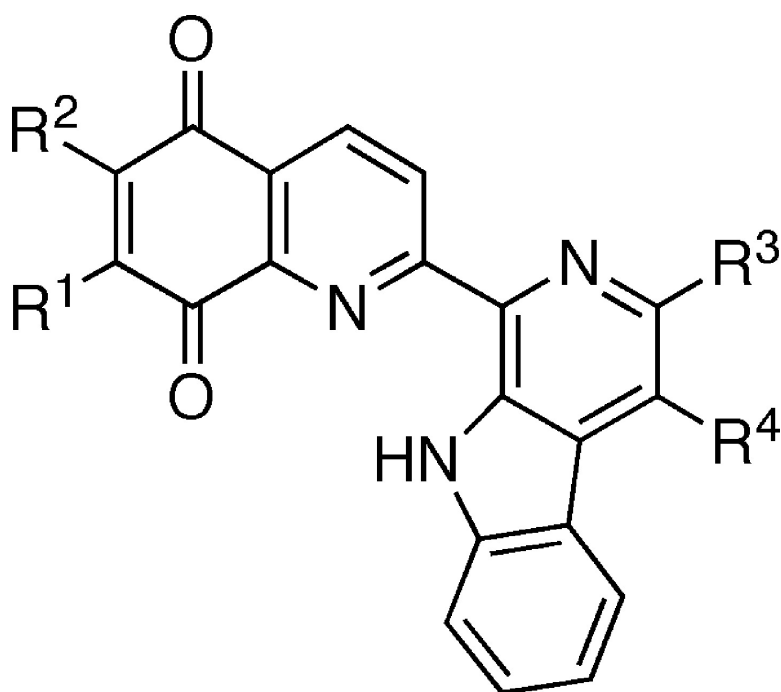


## Novel Lavendamycin Analogues as Antitumor Agents: Synthesis, in Vitro Cytotoxicity, Structure–Metabolism, and Computational Molecular Modeling Studies with NAD(P)H:Quinone Oxidoreductase 1

Mary Hassani, Wen Cai, David C. Holley, Jayana P. Lineswala, Babu R. Maharjan, G. Reza Ebrahimian, Hassan Seradj, Mark G. Stocksdale, Farahnaz Mohammadi, Christopher C. Marvin, John M. Gerdes, Howard D. Beall, and Mohammad Behforouz

*J. Med. Chem.*, **2005**, 48 (24), 7733-7749 • DOI: 10.1021/jm050758z • Publication Date (Web): 08 November 2005

Downloaded from <http://pubs.acs.org> on March 29, 2009



### More About This Article

Additional resources and features associated with this article are available within the HTML version:

- Supporting Information
- Links to the 4 articles that cite this article, as of the time of this article download
- Access to high resolution figures
- Links to articles and content related to this article



# Journal of Medicinal Chemistry

Subscriber access provided by American Chemical Society

- Copyright permission to reproduce figures and/or text from this article

[View the Full Text HTML](#)



**ACS Publications**  
High quality. High impact.

Journal of Medicinal Chemistry is published by the American Chemical Society, 1155  
Sixteenth Street N.W., Washington, DC 20036

# Novel Lavendamycin Analogues as Antitumor Agents: Synthesis, in Vitro Cytotoxicity, Structure–Metabolism, and Computational Molecular Modeling Studies with NAD(P)H:Quinone Oxidoreductase 1

Mary Hassani,<sup>†</sup> Wen Cai,<sup>‡</sup> David C. Holley,<sup>§</sup> Jayana P. Lineswala,<sup>‡</sup> Babu R. Maharjan,<sup>‡</sup> G. Reza Ebrahimian,<sup>‡</sup> Hassan Seradj,<sup>‡</sup> Mark G. Stocksdale,<sup>‡</sup> Farahnaz Mohammadi,<sup>‡</sup> Christopher C. Marvin,<sup>‡</sup> John M. Gerdes,<sup>§</sup> Howard D. Beall,<sup>\*,†</sup> and Mohammad Behforouz<sup>\*,‡</sup>

Department of Chemistry, Ball State University, Muncie, Indiana 47306, Center for Environmental Health Sciences, Department of Biomedical and Pharmaceutical Sciences, The University of Montana, Missoula, Montana 59812, and Molecular Computational Core Facility, Center for Structural and Functional Neuroscience and Department of Chemistry, The University of Montana, Missoula, Montana 59812

Received August 2, 2005

Novel lavendamycin analogues with various substituents were synthesized and evaluated as potential NAD(P)H:quinone oxidoreductase (NQO1)-directed antitumor agents. Pictet–Spengler condensation of quinoline- or quinoline-5,8-dione aldehydes with tryptamine or tryptophans yielded the lavendamycins. Metabolism studies with recombinant human NQO1 revealed that addition of NH<sub>2</sub> and CH<sub>2</sub>OH groups at the quinolinedione-7-position and indolopyridine-2'-position had the greatest positive impact on substrate specificity. The best and poorest substrates were **37** (2'-CH<sub>2</sub>OH-7-NH<sub>2</sub> derivative) and **31** (2'-CONH<sub>2</sub>-7-NHCOC<sub>3</sub>H<sub>7-n</sub> derivative) with reduction rates of 263 ± 30 and 0.1 ± 0.1 μmol/min/mg NQO1, respectively. Cytotoxicity toward human colon adenocarcinoma cells was determined for the lavendamycins. The best substrates for NQO1 were also the most selectively toxic to the NQO1-rich BE-NQ cells compared to NQO1-deficient BE-WT cells with **37** as the most selective. Molecular docking supported a model in which the best substrates were capable of efficient hydrogen-bonding interactions with key residues of the active site along with hydride ion reception.

## Introduction

The goal of current cancer drug discovery is to design cytotoxic compounds that selectively interact with molecular targets ideally unique to tumor cells with minimal toxicity to normal cells.<sup>1–3</sup> One approach to achieve selective toxicity is through bioreductive activation and identifying reductase enzymes that are overexpressed in tumor cells when compared to normal cells.<sup>1,3–5</sup> NAD(P)H:quinone oxidoreductase 1 (NQO1, DT-diaphorase, EC 1.6.99.2, DTD or QR1) is a widely distributed homodimeric flavoenzyme composed of two closely associated monomers of 273 residues, each containing one molecule of the noncovalently attached FAD cofactor molecule that is required for NQO1 catalytic activity.<sup>6–10</sup> This obligate two-electron reductase is present in cytosol (>90%)<sup>11</sup> and nucleus<sup>12</sup> and catalyzes a nicotinamide nucleotide-dependent two-electron reduction<sup>13,14</sup> and the bioactivation of quinone chemotherapeutic compounds such as mitomycins, indoloquinones, anthracyclines, and aziridinylbenzoquinones.<sup>15–19</sup> Marked elevations in NQO1 activity and mRNA content in primary tumors from lung, liver, colon and breast,<sup>20</sup> and lung,<sup>21</sup> liver,<sup>22</sup> brain,<sup>23</sup> and colorectal<sup>24</sup>

tumors suggest that antitumor compounds that are bioactivated by NQO1 may be selectively toxic to those tumors.

The crystal structure of the apo recombinant human NQO1 has been determined to a resolution of 1.7 Å.<sup>9</sup> Each monomer of the physiological dimer of NQO1 is composed of two distinct domains such that residues 1–220 and 221–273 form a major catalytic and a small C-terminal domain, respectively.<sup>9,10,25,26</sup> Two equivalent active sites are located at the dimer interface and are formed by portions of both subunits.<sup>6,9</sup> The active site of the enzyme is a hydrophobic and plastic pocket with three potential hydrogen-bonding residues (Tyr-126 and -128 and His-161) that can bind and accommodate a broad range of structures including large quinone compounds.<sup>9,25</sup> The substrate binding pocket (360 Å<sup>3</sup>) sequentially binds NAD(P)H and the quinone substrate and is formed by residues from both monomers.<sup>9,10,25</sup>

NQO1 promotes an obligatory two-electron reduction called a ping-pong mechanism such that in the first half of the reaction a hydride ion from NAD(P)H is transferred to the N5 of the FAD followed by the release of NAD(P)<sup>+</sup>.<sup>10,27,28</sup> The hydride donation from the FADH<sub>2</sub> N5 to the hydride-acceptor substrate (across a 4 Å distance<sup>28</sup>) can then be done at either a carbonyl oxygen or ring carbon followed by hydroquinone release. The remaining proton can be provided by Tyr-126, -128, or His-161.<sup>10,27,28</sup> Quinone substrates can bind to the NQO1 active site in more than one orientation, and homologous compounds with different substituents may bind to the NQO1 active site in different orientations.<sup>25,27</sup>

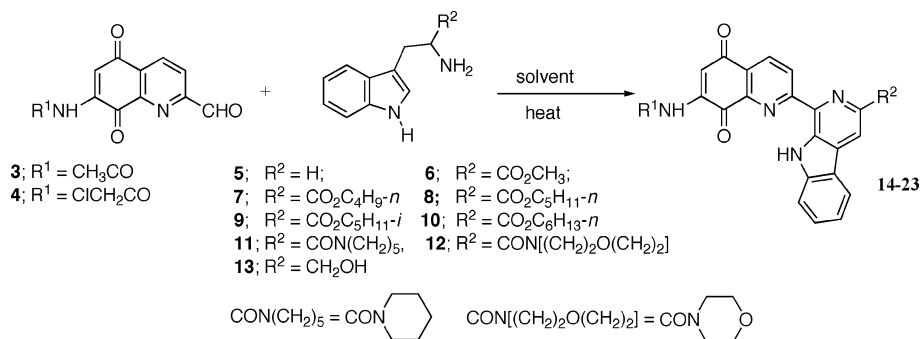
\* Corresponding authors for chemistry (M.B.) and biology (H.D.B.): M. Behforouz: Phone, 765-285-8070; Fax, 765-285-6505; E-mail, mbehforo@bsu.edu. H. D. Beall: Phone, 406-243-5112; Fax, 406-243-5228; E-mail, howard.beall@umontana.edu.

<sup>‡</sup> Department of Chemistry, Ball State University.

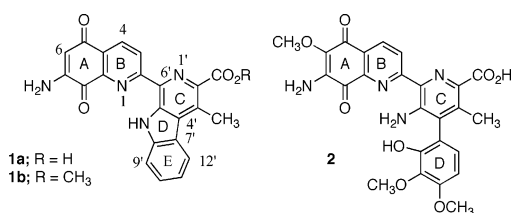
<sup>†</sup> Center for Environmental Health Sciences, The University of Montana.

<sup>§</sup> Molecular Computational Core Facility, The University of Montana.

## Scheme 1



Lavendamycin (**1a**), a bacterially derived quinolinedione antibiotic, was isolated from the fermentation broth of *Streptomyces lavendulae* in 1981.<sup>29</sup> Lavendamycin is structurally<sup>29,30</sup> and biosynthetically<sup>31–33</sup> related to streptonigrin (SN) (**2**), another potent 7-aminoquinoline-



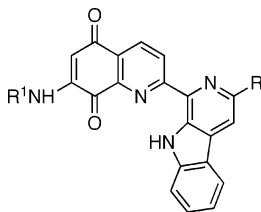
5,8-dione antitumor antibiotic. Earlier work has shown that the use of both of these antitumor agents as potential drugs has been precluded due to their high degree of toxicity.<sup>30,34,35</sup> However, in contrast to the parent compound, we have found that a significant number of lavendamycin derivatives have low animal toxicity but show strong antitumor activity or are potent inhibitors of the HIV-reverse transcriptase.<sup>36–38</sup> These studies have been possible only through our success in developing short and efficient syntheses for a variety of lavendamycin analogues possessing the full pentacyclic structure. For instance, compared to the previously reported syntheses of lavendamycin ester (**1b**) in overall yields of 0.5 to 2% and in 9 to 20 steps,<sup>39,40</sup> we were able to synthesize **1b** in 5-step methods<sup>41,42</sup> with overall yields of nearly 40%.

This study was conducted to clarify the role of NQO1 in the bioactivation of lavendamycin analogues. Specifically, the objectives were to analyze the effects of functional group changes on the reduction efficiency of lavendamycin analogues by NQO1, to verify whether activation by NQO1 resulted in selective cytotoxicity of these compounds and to correlate the metabolism and biological data of the compounds with predictions of their active site positioning, hydrogen bond formation, and hydride ion reception capability. For this study, we were in need of a large number of variously substituted lavendamycins possessing zero to four substituents on their pentacyclic system for which their syntheses are described below. Additionally, the synthesis of a number of quinolinediones is reported.

## Results and Discussion

**Synthetic Chemistry.** A range of lavendamycin analogues was designed and synthesized to explore the effects of various substituents on the metabolism of

**Table 1.** Structures of Lavendamycin Analogues, Reaction Conditions and Yields



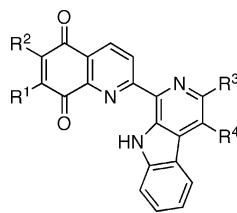
no.	R <sup>1</sup>	R <sup>2</sup>	% yield	solvent	h (°C) <sup>a</sup>
<b>14</b>	CH <sub>3</sub> CO	H	83	anisole	5 (reflux)
<b>15</b>	CH <sub>3</sub> CO	CO <sub>2</sub> CH <sub>3</sub>	67	anisole	4.5 (reflux)
<b>16</b>	CH <sub>3</sub> CO	CO <sub>2</sub> C <sub>4</sub> H <sub>9</sub> - <i>n</i>	63	xylene	4 (reflux)
<b>17</b>	CH <sub>3</sub> CO	CO <sub>2</sub> C <sub>5</sub> H <sub>11</sub> - <i>n</i>	44	xylene	4.5 (reflux)
<b>18</b>	CH <sub>3</sub> CO	CO <sub>2</sub> C <sub>5</sub> H <sub>11</sub> - <i>i</i>	50	xylene	9.5 (28–130)
<b>19</b>	CH <sub>3</sub> CO	CO <sub>2</sub> C <sub>6</sub> H <sub>13</sub> - <i>n</i>	54	xylene	5.5 (reflux)
<b>20</b>	CH <sub>3</sub> CO	CO-piperidino	56	anisole	17 (reflux)
<b>21</b>	CH <sub>3</sub> CO	CO-morpholino	57	anisole	18 (reflux)
<b>22</b>	CH <sub>3</sub> CO	CH <sub>2</sub> OH	48	anisole	4 (25–155)
<b>23</b>	ClCH <sub>2</sub> CO	CO <sub>2</sub> C <sub>5</sub> H <sub>11</sub> - <i>i</i>	57	xylene	5 (76)

<sup>a</sup> Except for compounds **18**, **22** and **23** the reaction mixtures were slowly heated to reflux over a period of approximately 3 h and then refluxed for the designated times.

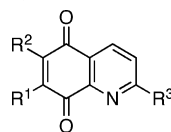
these analogues by recombinant human NQO1. Pictet–Spengler condensation (Scheme 1) of 7-*N*-acylamino-2-formylquinoline-5,8-diones **3** or **4** with tryptamine, or derivatives of tryptophan or  $\beta$ -methyltryptophan (**5**–**13**), yielded lavendamycin analogues **14**–**23**.

In a typical procedure, aldehydes **3** or **4** (0.1 mmol) were mixed with the corresponding tryptamine or tryptophan derivatives in dry anisole or xylene under argon, and while being magnetically stirred, the mixture was gradually heated to reflux over a period of 3 h.<sup>38,41,42</sup> The resulting clear solution was refluxed until TLC showed the absence of the starting materials. The mixture was concentrated or evaporated to dryness. The products were either precipitated from the concentrated solutions or purified by washing with solvents. The structures of the resulting lavendamycins, the reaction conditions, and the yields are shown in Table 1. Table 2 presents the structures of a number of other novel lavendamycins as well as some of our previously synthesized derivatives. Table 3 lists the structures of quinolinediones. The lavendamycin analogues shown in the tables are the subject of the biological tests in this study.

Following Scheme 2, aldehydes **3** and **43** were prepared according to our reported syntheses.<sup>38,41,42</sup> Aldehyde **4** was obtained by the reduction of **47**, then chloroacetylation of the resulting amino salt followed by two consecutive oxidations.

**Table 2.** Structures of Lavendamycin Analogues

no.	R <sup>1</sup>	R <sup>2</sup>	R <sup>3</sup>	R <sup>4</sup>	refs
<b>24</b>	CH <sub>3</sub> CONH	pyrrolidino	CO <sub>2</sub> CH <sub>3</sub>	CH <sub>3</sub>	
<b>25</b>	CH <sub>3</sub> CONH	aziridino	CONH <sub>2</sub>	H	
<b>26</b>	CH <sub>3</sub> CONH	H	CO <sub>2</sub> CH <sub>3</sub>	CH <sub>3</sub>	41, 42
<b>27</b>	CH <sub>3</sub> CONH	H	CO <sub>2</sub> C <sub>8</sub> H <sub>17-n</sub>	H	38
<b>28</b>	CH <sub>3</sub> CONH	H	CO <sub>2</sub> (CH <sub>2</sub> ) <sub>2</sub> OH	H	38
<b>29</b>	CH <sub>3</sub> CONH	H	CO <sub>2</sub> (CH <sub>2</sub> ) <sub>2</sub> OPO <sub>3</sub> H <sub>2</sub>	H	38
<b>30</b>	CH <sub>3</sub> CONH	H	CONH <sub>2</sub>	H	38
<b>31</b>	<i>n</i> -C <sub>3</sub> H <sub>7</sub> CONH	H	CONH <sub>2</sub>	H	38
<b>32</b>	NH <sub>2</sub>	Cl	CO <sub>2</sub> CH <sub>3</sub>	CH <sub>3</sub>	
<b>33</b>	NH <sub>2</sub>	H	CO <sub>2</sub> CH <sub>3</sub>	CH <sub>3</sub>	41, 42
<b>34</b>	Br	H	CO <sub>2</sub> CH <sub>3</sub>	CH <sub>3</sub>	
<b>35</b>	NH <sub>2</sub>	H	CO <sub>2</sub> C <sub>8</sub> H <sub>17-n</sub>	H	38
<b>36</b>	NH <sub>2</sub>	H	CONH <sub>2</sub>	H	38
<b>37</b>	NH <sub>2</sub>	H	CH <sub>2</sub> OH	H	
<b>38</b>	NH <sub>2</sub>	H	H	H	
<b>39</b>	H	H	H	H	

**Table 3.** Structures of Quinoline-5,8-diones

no.	R <sup>1</sup>	R <sup>2</sup>	R <sup>3</sup>	refs
<b>3</b>	CH <sub>3</sub> CONH	H	CHO	41, 42
<b>4</b>	ClCH <sub>2</sub> CONH	H	CHO	
<b>40</b>	CH <sub>3</sub> CONH	H	CH <sub>3</sub>	41, 42
<b>41</b>	ClCH <sub>2</sub> CONH	H	CH <sub>3</sub>	
<b>42</b>	<i>n</i> -C <sub>3</sub> H <sub>7</sub> CONH	H	CH <sub>3</sub>	38
<b>43</b>	<i>n</i> -C <sub>3</sub> H <sub>7</sub> CONH	H	CHO	38
<b>44</b>	NH <sub>2</sub>	H	CH <sub>3</sub>	38
<b>45</b>	NH <sub>2</sub>	Cl	CH <sub>3</sub>	38
<b>46</b>	NH <sub>2</sub>	Cl	CHO	

Tryptamine (**5**) is commercially available and tryptophans **6**, **7** and **13** were obtained by the neutralization of the commercially available salts with ammonia (14%) and extraction with ethyl acetate. Tryptophan esters **8–10** were prepared by the Fischer esterification of the tryptophans with the corresponding alcohols.  $\beta$ -Methyltryptophan methyl ester necessary for the synthesis of **32** and **57**, the precursor of **34** was prepared according to our own reported procedure.<sup>43</sup>

Chloroaldehyde **46** was obtained following the chemistry in Scheme 3.<sup>44</sup>

The 6-substituted pyrrolidino and aziridino lavendamycins were synthesized by an efficient Michael addition of the amines to the corresponding lavendamycins in excellent yields according to Scheme 4.<sup>45</sup>

Amino analogues **37** and **38** were prepared by the acid hydrolysis of acetyl derivatives **22** and **14** in high yields as shown in Scheme 5.

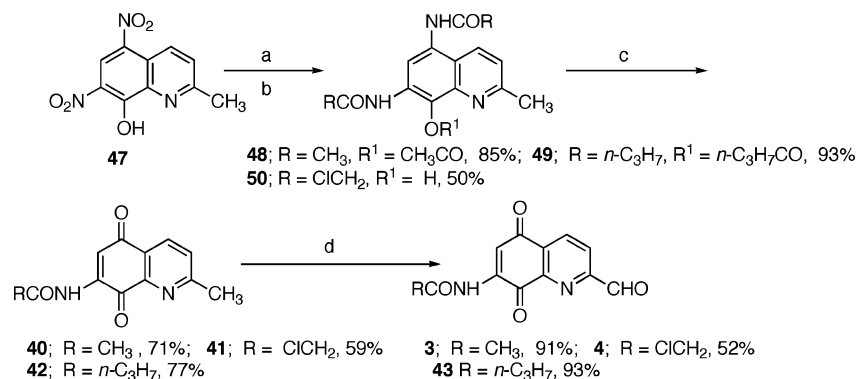
Bromo analogue **34** and unsubstituted lavendamycin **39** were synthesized following the reactions presented in Scheme 6. Quinoline aldehydes **55** and **56** were synthesized by the selenium dioxide oxidation of the commercially available **53** and **54** followed by the condensation with  $\beta$ -methyltryptophan methyl ester or

tryptamine to produce **57** and **58** which then oxidized by bis[(trifluoroacetoxy)iodo]benzene<sup>46</sup> to the products.

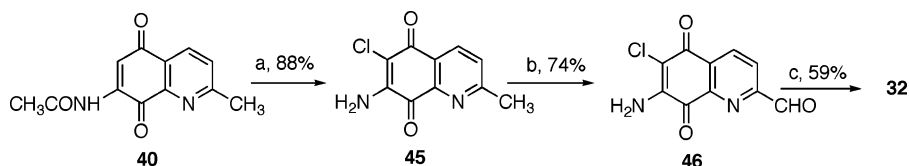
Scheme 7 presents the steps in the synthesis of the desired piperidine and morpholine amides of tryptophan. Tryptophans **11** and **12** were prepared in relatively good yields by a method similar to that of Tolstikov used for the synthesis of streptonigrin derivatives.<sup>47</sup>

**Electrochemistry.** The aim of the electrochemical studies was to determine the relative ease of reduction of the lavendamycin analogues and to compare how the electrochemical behavior of these compounds correlates with their reduction rate by NQO1. Electrochemical studies of a number of lavendamycin analogues were carried out. In these studies, dried dimethyl sulfoxide (DMSO) and tetrabutylammonium hexafluorophosphate (Bu<sub>4</sub>NPF<sub>6</sub>) were used as solvent and the supporting electrolyte, respectively. Cathodic and anodic peak potentials,  $E_{pc}$  and  $E_{pa}$ , respectively, were measured and the midpoint of the peak potentials was used to determine  $E_{1/2}$  values,  $E_{1/2} = (E_{pc} + E_{pa})/2$ .  $E_{1/2}$  values were consistent for the potential sweep rates in the range of 50 to 500 mV/s. The  $E_{1/2}$  values determined from the recorded voltammograms at the potential sweep rates of 50, 100, 200, 400, and 500 mV/s were averaged and reported with reference to ferrocene (Fc<sup>0/+</sup>)  $E_{1/2}$  value (Table 4).

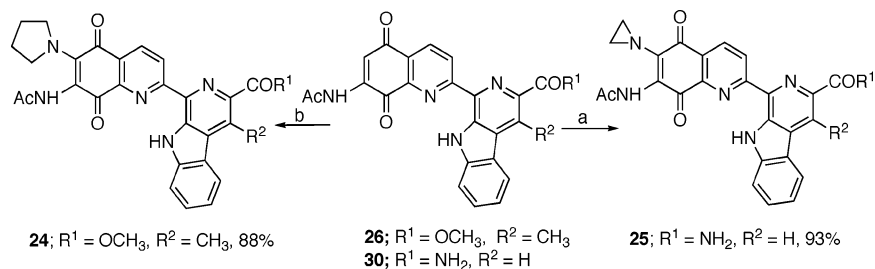
All of the lavendamycin analogues exhibited reversible electrochemistry. The analogues with electron-withdrawing groups at the R<sup>1</sup> position showed similar  $E_{1/2}$  values, between  $-0.85$  and  $-0.99$  V, with the exception of compound **24** that exhibited a slightly more negative  $E_{1/2}$  value which can be in part due to the presence of an electron-donating group at the R<sup>2</sup> position (Table 4). The lavendamycin analogues with electron-donating groups at the R<sup>1</sup> position showed slightly more negative  $E_{1/2}$  values, between  $-1.01$  and  $-1.09$  V, compared to the former group (Table 4). In general, the lavendamycin analogues with electron-withdrawing groups at the R<sup>1</sup> position were easier to reduce compared to the ones with electron-donating groups at this position. Although all of the investigated lavendamycin analogues possessed similar  $E_{1/2}$  values ( $-0.85$  to  $-1.13$  V) (Table 4), the rate of reduction of these compounds by NQO1 differed dramatically (Table 5). When the electrochemical reduction potential and rate of reduction of the lavendamycin analogues by NQO1 were compared, no direct correlation between the two factors was found (data not shown). This finding along with our molecular modeling studies suggest that other factors such as lavendamycins substituent size, steric influence, active site positioning, and hydrogen bond formation capability may be more important than the electrochemical reduction potential and electronic effects to determine the reduction efficiency of these compounds by NQO1. Electrochemical studies can be used to determine the ease of reduction of compounds, but there is often no overall or very small association between the rate of reduction by NQO1 and reduction potential for quinones such as indolequinones<sup>48–50</sup> and quinolinequinones<sup>51</sup> as previously reported. The lavendamycin analogues exhibited similar reduction potential values to the quinolinequinone compounds studied by Fryatt et al.<sup>51</sup> Also, they were easier to reduce ( $E_{1/2}$  values =  $-0.85$  to  $-1.13$  V) than the indolequinones previously

Scheme 2<sup>a</sup>

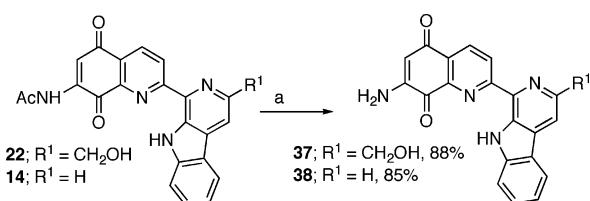
<sup>a</sup> Reagents and conditions: (a) Pd-C, 5%, H<sub>2</sub> (30 psi), HCl-H<sub>2</sub>O, 15 h, rt; (b) (RCO)<sub>2</sub>O, NaOAc, Na<sub>2</sub>SO<sub>3</sub>, 2.5 h, rt to 0 °C; (c) K<sub>2</sub>Cr<sub>2</sub>O<sub>7</sub>, HOAc, 12 h, rt; (d) SeO<sub>2</sub>, dioxane, H<sub>2</sub>O, 9–29.5 h, reflux.

Scheme 3<sup>a</sup>

<sup>a</sup> Reagents and conditions: (a) HCl (gas), dry MeOH, 22 h, 60 °C; (b) SeO<sub>2</sub>, dioxane, H<sub>2</sub>O, 23 h, reflux; (c) β-methyltryptophan methyl ester, anisole, 3 h, rt to 130 °C, then 1 h, reflux.

Scheme 4<sup>a</sup>

<sup>a</sup> Reagents and conditions: (a) aziridine, CHCl<sub>3</sub>, 48 h, rt; (b) pyrrolidine, CHCl<sub>3</sub>, 2 h, rt.

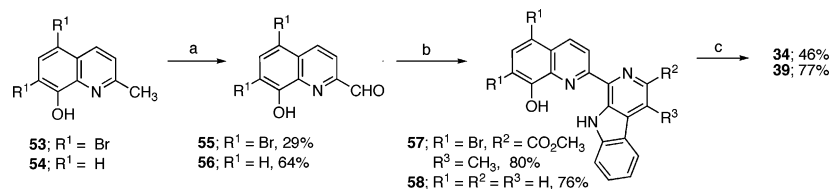
Scheme 5<sup>a</sup>

<sup>a</sup> Reagents and conditions: (a) H<sub>2</sub>SO<sub>4</sub> (70%), 2–4 h, 60 °C.

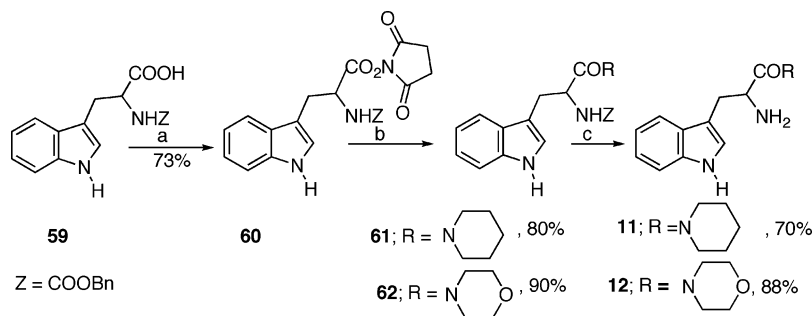
studied by Beall et al. and Swann et al. ( $E_{1/2}$  values = -1.19 to -1.61 V).<sup>49,50</sup>

**Biological Studies.** Metabolism of the novel lavendamycin analogues by recombinant human NQO1 and cytotoxicity to human colon adenocarcinoma cells with either no detectable NQO1 activity (BE-WT) or with high NQO1 activity (BE-NQ) were examined. The effect of functional group changes on reduction efficiency and rate of reduction by NQO1 was studied using a spectrophotometric assay that employs cytochrome *c* as the terminal electron acceptor<sup>52</sup> and gives initial rates of lavendamycin analogues reduction (Table 5). The initial reduction rates ( $\mu\text{mol}$  cytochrome *c* reduced/min/mg NQO1) were calculated from the linear portion (0–30 s) of the reaction graphs.

Large substituents at the quinolinedione-7-position (R<sup>1</sup>) of the lavendamycin analogues were poorly tolerated and greatly reduced the metabolism rate of the analogues by NQO1 compared to smaller substituents (31 vs 36, 18 vs 23, and 30 vs 31) (Table 5). Large substituents such as NHCOC<sub>3</sub>H<sub>7</sub>-*n* in 31 at the 7-position had the most negative impact on the rate of reduction by NQO1 whereas NH<sub>2</sub> followed by the NHCOC<sub>3</sub>H<sub>7</sub> group were the best substituents for this position (Table 5). This could partly be due to steric hindrance between the quinolinedione moiety (5,8-dione ring enters the active site first) and NQO1 active site that results in unfavorable positioning of the lavendamycin analogues for hydride ion reception from FADH<sub>2</sub> and quinone reduction. Our molecular modeling studies also demonstrated that placing a small substituent at the R<sup>1</sup> position that is capable of hydrogen bonding with key residues of the active site could be a contributing factor to substrate specificity. Faig et al. determined that positions of 63 (RH1), 2,5-diaziridinyl-3-(hydroxymethyl)-6-methyl-1,4-benzoquinone,<sup>53</sup> that point to the inner part of the NQO1 active site could accommodate only small substituents.<sup>25</sup> Also, 1,4-naphthoquinones with small substituents such as an aziridine ring or CH<sub>3</sub> at C2 and no substituents at C3 were reported to be

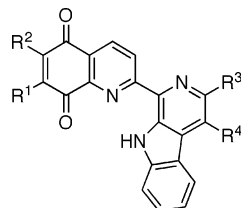
Scheme 6<sup>a</sup>

<sup>a</sup> Reagents and conditions: (a) SeO<sub>2</sub>, wet dioxane, 2 h, rt to reflux, then 17–22 h, reflux; (b) tryptamine or β-methyltryptophan methyl ester, anisole, 3 h, rt to reflux, then 22–39 h, reflux, then Pd–C, 5%, 28 h, reflux; (c) Bis[(trifluoroacetoxy)iodo]benzene, CH<sub>3</sub>CN–H<sub>2</sub>O, 2 h, 0 °C.

Scheme 7<sup>a</sup>

<sup>a</sup> Reagents and conditions: (a) *N*-hydroxysuccinimide, DCC, 2 h, 12–20 °C, dioxane (b) amine, Et<sub>3</sub>N, EtOH, CH<sub>3</sub>Cl, rt, 1 h (c) dry ammonium formate, Pd–C, 10%, dry methanol, rt, 30 min.

**Table 4.** Electrochemical Reduction Potentials<sup>a</sup> (DMSO) of Lavendamycin Analogues versus Ferrocene



no.	R <sup>1</sup>	R <sup>2</sup>	R <sup>3</sup>	R <sup>4</sup>	<i>E</i> <sub>pc</sub> (V)	<i>E</i> <sub>pa</sub> (V)	<i>E</i> <sub>1/2</sub> (V) vs Fc
14	CH <sub>3</sub> CONH	H	H	H	–0.95	–0.95	–0.95
15	CH <sub>3</sub> CONH	H	CO <sub>2</sub> CH <sub>3</sub>	H	–0.92	–0.83	–0.88
24	CH <sub>3</sub> CONH	pyrrolidino	CO <sub>2</sub> CH <sub>3</sub>	CH <sub>3</sub>	–1.16	–1.10	–1.13
25	CH <sub>3</sub> CONH	aziridino	CONH <sub>2</sub>	H	–0.99	–0.93	–0.96
26	CH <sub>3</sub> CONH	H	CO <sub>2</sub> CH <sub>3</sub>	CH <sub>3</sub>	–0.91	–0.85	–0.88
28	CH <sub>3</sub> CONH	H	CO <sub>2</sub> (CH <sub>2</sub> ) <sub>2</sub> OH	H	–1.02	–0.95	–0.99
30	CH <sub>3</sub> CONH	H	CONH <sub>2</sub>	H	–0.88	–0.82	–0.85
31	<i>n</i> -C <sub>3</sub> H <sub>7</sub> CONH	H	CONH <sub>2</sub>	H	–0.92	–0.89	–0.91
32	NH <sub>2</sub>	Cl	CO <sub>2</sub> CH <sub>3</sub>	CH <sub>3</sub>	–1.01	–1.01	–1.01
33	NH <sub>2</sub>	H	CO <sub>2</sub> CH <sub>3</sub>	CH <sub>3</sub>	–1.10	–1.04	–1.07
36	NH <sub>2</sub>	H	CONH <sub>2</sub>	H	–1.09	–1.05	–1.07
37	NH <sub>2</sub>	H	CH <sub>2</sub> OH	H	–1.11	–1.06	–1.09
38	NH <sub>2</sub>	H	H	H	–1.12	–1.06	–1.09
39	H	H	H	H	–0.88	–0.85	–0.87

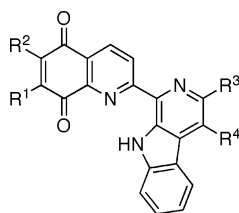
<sup>a</sup> *E*<sub>1/2</sub> values (± 0.005 V) calculated as (*E*<sub>pc</sub> + *E*<sub>pa</sub>)/2 are averages of the values determined from voltammograms recorded at potential sweep rates of 50, 100, 200, 300, 400 and 500 mV/s; *E*<sub>pc</sub> = cathodic peak potential; *E*<sub>pa</sub> = anodic peak potential.

good substrates for NQO1.<sup>54</sup> Dipyrroloimidazobenzimidazole compounds with both pyrrolo rings bearing bulky substituents were determined to be poor substrates for NQO1 due to steric interactions with residues of the NQO1 active site.<sup>55</sup>

Comparison of analogues **32** vs **33** and **25** vs **30** determined that 6-unsubstituted (R<sup>2</sup>) lavendamycin analogues are far better substrates for NQO1 than the corresponding 6-substituted counterparts (Table 5). This is likely due to active site constraints and steric effects caused by substituents that hinder entrance or proper positioning of the 5,8-dione moiety of the analogues toward the key residues of the active site and the FAD isalloxazine ring for hydride ion reception and quin-

one reduction. This finding is consistent with other studies that previously showed that increased bulkiness of the substituents at C5 position on **64** (EO9), 3-hydroxy-5-aziridinyl-1-methyl-2-(1*H*-indole-4,7-dione)-propenol,<sup>56</sup> dramatically reduced rates of reduction by NQO1.<sup>25,52</sup> Another study determined that indolequinones and mitosenes with bulky amine substituents at C5 and C7 positions, respectively, are not substrates for NQO1 due to steric effects.<sup>49</sup>

A number of substituents at the 2'-position of the fused indolopyridine moiety (R<sup>3</sup>) were also investigated. Among the analogues that shared an NH<sub>2</sub> group at the R<sup>1</sup> position and had no substituent at R<sup>2</sup>, 2'-CH<sub>2</sub>OH derivative (**37**) was the best substrate followed by the

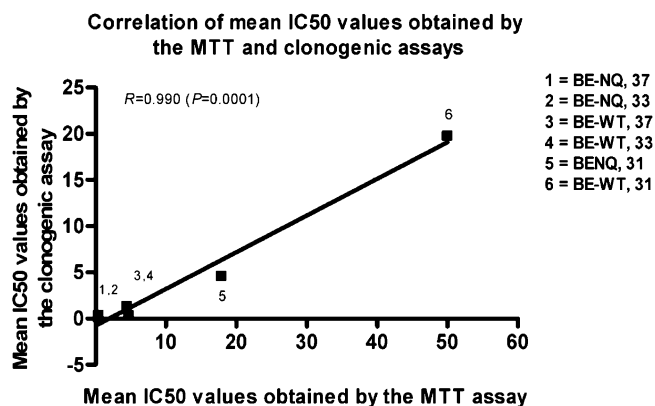
**Table 5.** Metabolism of Lavendamycin Analogues by Recombinant Human NQO1 Monitored by Spectrophotometric Cytochrome *c* Assay

no.	R <sup>1</sup>	R <sup>2</sup>	R <sup>3</sup>	R <sup>4</sup>	metabolism by NQO1 ( $\mu\text{mol}/\text{min}/\text{mg}$ ) (cytochrome <i>c</i> reduction)
14	CH <sub>3</sub> CONH	H	H	H	2.7 ± 1.2
15	CH <sub>3</sub> CONH	H	CO <sub>2</sub> CH <sub>3</sub>	H	0.9 ± 0.2
16	CH <sub>3</sub> CONH	H	CO <sub>2</sub> C <sub>4</sub> H <sub>9</sub> - <i>n</i>	H	8.6 ± 2.6
17	CH <sub>3</sub> CONH	H	CO <sub>2</sub> C <sub>5</sub> H <sub>11</sub> - <i>n</i>	H	9.2 ± 6.6
18	CH <sub>3</sub> CONH	H	CO <sub>2</sub> C <sub>5</sub> H <sub>11</sub> - <i>i</i>	H	35.4 ± 6.9
19	CH <sub>3</sub> CONH	H	CO <sub>2</sub> C <sub>6</sub> H <sub>13</sub> - <i>n</i>	H	11.7 ± 5.3
20	CH <sub>3</sub> CONH	H	CO-piperidino	H	15.2 ± 11.5
21	CH <sub>3</sub> CONH	H	CO-morpholino	H	7.5 ± 1.5
23	ClCH <sub>2</sub> CONH	H	CO <sub>2</sub> C <sub>5</sub> H <sub>11</sub> - <i>i</i>	H	9.9 ± 5.6
24	CH <sub>3</sub> CONH	pyrrolidino	CO <sub>2</sub> CH <sub>3</sub>	CH <sub>3</sub>	1 ± 1
25	CH <sub>3</sub> CONH	aziridino	CONH <sub>2</sub>	H	0.2 ± 0.2
26	CH <sub>3</sub> CONH	H	CO <sub>2</sub> CH <sub>3</sub>	CH <sub>3</sub>	1.9 ± 1.7
27	CH <sub>3</sub> CONH	H	CO <sub>2</sub> C <sub>8</sub> H <sub>17</sub> - <i>n</i>	H	1.5 ± 0.8
28	CH <sub>3</sub> CONH	H	CO <sub>2</sub> (CH <sub>2</sub> ) <sub>2</sub> OH	H	11.0 ± 2.5
29	CH <sub>3</sub> CONH	H	CO <sub>2</sub> (CH <sub>2</sub> ) <sub>2</sub> OPO <sub>3</sub> H <sub>2</sub>	H	15.4 ± 0.9
30	CH <sub>3</sub> CONH	H	CONH <sub>2</sub>	H	33 ± 12
31	<i>n</i> -C <sub>3</sub> H <sub>7</sub> CONH	H	CONH <sub>2</sub>	H	0.1 ± 0.1
32	NH <sub>2</sub>	Cl	CO <sub>2</sub> CH <sub>3</sub>	CH <sub>3</sub>	0.9 ± 0.8
33	NH <sub>2</sub>	H	CO <sub>2</sub> CH <sub>3</sub>	CH <sub>3</sub>	21 ± 12
34	Br	H	CO <sub>2</sub> CH <sub>3</sub>	CH <sub>3</sub>	0.7 ± 0.3
35	NH <sub>2</sub>	H	CO <sub>2</sub> C <sub>8</sub> H <sub>17</sub> - <i>n</i>	H	106 ± 15
36	NH <sub>2</sub>	H	CONH <sub>2</sub>	H	18.3 ± 13.6
37	NH <sub>2</sub>	H	CH <sub>2</sub> OH	H	263 ± 30
38	NH <sub>2</sub>	H	H	H	24.0 ± 6.5
39	H	H	H	H	3.4 ± 1.2

2'-CO<sub>2</sub>C<sub>8</sub>H<sub>17</sub>-*n* derivative (**35**) (Table 5). Molecular modeling demonstrated that the CH<sub>2</sub>OH group at R<sup>3</sup> was capable of hydrogen bond formation with the key residues of the NQO1 active site and therefore could be an important contributing factor to substrate specificity. A CH<sub>2</sub>OH group at the C6 position of a series of substituted 1,4-naphthoquinones also contributed the most to substrate specificity for NQO1.<sup>54</sup> Phillips et al. determined that some of the good indolequinone substrates for NQO1 including **64** possessed a CH<sub>2</sub>OH group at the analogous C3 position.<sup>52</sup> Furthermore, **63**, which is an excellent substrate for NQO1, possesses a CH<sub>2</sub>OH group at C3 position.<sup>7,53</sup>

Addition of NH<sub>2</sub> and CH<sub>2</sub>OH groups at R<sup>1</sup> and R<sup>3</sup> positions, respectively, had the greatest positive impact on substrate specificity compared to other substituents at these positions. The best substrate was the 2'-CH<sub>2</sub>-OH-7-NH<sub>2</sub> derivative (**37**) with a reduction rate of 263 ± 30  $\mu\text{mol}/\text{min}/\text{mg}$  NQO1 (Table 5). These findings enhance our understanding of the relationship between lavendamycin structure and rates of reduction by NQO1.

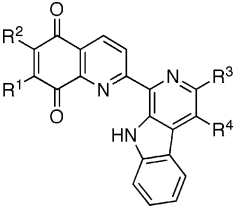
Cytotoxicity studies were also performed on representative lavendamycins with cell survival being determined by colorimetric MTT and clonogenic assays. We used the BE human colon adenocarcinoma cells stably transfected with human NQO1 cDNA.<sup>53</sup> The BE cells (BE-WT) had no measurable NQO1 activity whereas activity in the transfected cells (BE-NQ) was greater than 660 nmol/min/mg total cell protein using dichlorophenolindophenol as the standard electron acceptor.



**Figure 1.** Correlation of mean IC<sub>50</sub> values obtained by the MTT and clonogenic assays. The mean IC<sub>50</sub> values obtained by the MTT assay were plotted along the horizontal axis and mean IC<sub>50</sub> values obtained by the clonogenic assay were plotted along the vertical axis. The correlation coefficient was 0.990 ( $P = 0.0001$ ).

We also evaluated the correlation between the chemosensitivity results of clonogenic and MTT assays in both cell lines for three lavendamycin analogues, **31**, **33**, and **37**. There was an excellent positive linear correlation between the IC<sub>50</sub> values of the two assays for the three lavendamycins for BE-WT ( $r = 0.999$ ,  $P = 0.03$ ), BE-NQ ( $r = 0.999$ ,  $P = 0.025$ ) and both cell lines ( $r = 0.990$ ,  $P = 0.0001$ ) (Figure 1). In this study the cytotoxicity of representative lavendamycin analogues (Table 6) has been compared using these cell lines.



**Table 6.** Cytotoxicity of Lavendamycin Analogues toward BE-WT (NQO1-deficient) and BE-NQ (NQO1-rich) Human Colon Adenocarcinoma Cell Lines


no.	R <sup>1</sup>	R <sup>2</sup>	R <sup>3</sup>	R <sup>4</sup>	cytotoxicity IC <sub>50</sub> (μM)		selectivity ratio [IC <sub>50</sub> (BE-WT)/IC <sub>50</sub> (BE-NQ)]
					BE-NQ	BE-WT	
<b>16</b>	CH <sub>3</sub> CONH	H	CO <sub>2</sub> C <sub>4</sub> H <sub>9-n</sub>	H	20.5 ± 0.6	20.0 ± 2.3	1.0
<b>26</b>	CH <sub>3</sub> CONH	H	CO <sub>2</sub> CH <sub>3</sub>	CH <sub>3</sub>	13.2 ± 0.7	19.3 ± 4.3	1.5
<b>27</b>	CH <sub>3</sub> CONH	H	CO <sub>2</sub> C <sub>8</sub> H <sub>17-n</sub>	H	>50	>50	-
<b>29</b>	CH <sub>3</sub> CONH	H	CO <sub>2</sub> (CH <sub>2</sub> ) <sub>2</sub> OPO <sub>3</sub> H <sub>2</sub>	H	6.8 ± 0.6	8.1 ± 0.5	1.2
<b>30</b>	CH <sub>3</sub> CONH	H	CONH <sub>2</sub>	H	0.8 ± 0.0	3.5 ± 0.7	4.4
<b>31</b>	<i>n</i> -C <sub>3</sub> H <sub>7</sub> CONH	H	CONH <sub>2</sub>	H	21.4 ± 1.2	>50	2.3
<b>33</b>	NH <sub>2</sub>	H	CO <sub>2</sub> CH <sub>3</sub>	CH <sub>3</sub>	0.5 ± 0.1	4.7 ± 0.7	9.4
<b>34</b>	Br	H	CO <sub>2</sub> CH <sub>3</sub>	CH <sub>3</sub>	>50	>50	-
<b>35</b>	NH <sub>2</sub>	H	CO <sub>2</sub> C <sub>8</sub> H <sub>17-n</sub>	H	3.4 ± 0.7	35.0 ± 3.4	10.3
<b>36</b>	NH <sub>2</sub>	H	CONH <sub>2</sub>	H	0.2 ± 0.0	1.8 ± 0.1	9.0
<b>37</b>	NH <sub>2</sub>	H	CH <sub>2</sub> OH	H	0.4 ± 0.1	4.5 ± 0.2	11.3
<b>38</b>	NH <sub>2</sub>	H	H	H	8.0 ± 0.5	16.8 ± 1.0	2.1
<b>39</b>	H	H	H	H	12.4 ± 1.0	9.3 ± 1.2	0.8

Lavendamycin analogues such as **30**, **33**, **35**, **36**, and **37** that were good substrates for NQO1 (Table 5) were also more toxic to the NQO1-rich cell line (BE-NQ) than the NQO1-deficient cell line (BE-WT) (Table 6). Compound **37**, the best substrate for NQO1 (Table 5), had the greatest differential toxicity with a selectivity ratio of 11 (Table 6). Antitumor and antiproliferative activity of lavendamycin against implanted leukemia cells in BDF1 mice and three other cancer cell lines has been previously reported.<sup>30,57</sup> A recent study investigating cytotoxic activities of a series of lavendamycin analogues against A549 human lung carcinoma cells indicated that compounds with an amide or amine substituent at the R<sup>3</sup> position displayed the most potent colony formation inhibitory effects.<sup>36</sup> At a concentration of 10 nM, the most potent compound of this group, MB-97, reduced the colony outgrowth of A549 cells by 70%.<sup>36</sup> Since MB-97 also displayed promising cytotoxic and antitumor activities in the NCI's 60-cell line panel and in vivo hollow fiber tumorigenesis assay, it has been considered for in vivo testing against tumor xenografts in mice.<sup>36</sup> Our study also determined that compound **36** (MB-97) showed highly selective toxicity toward BE-NQ cells (selectivity ratio = 9). Lavendamycin analogues such as **26**, **27**, **31**, **34**, and **39** that were poor substrates for NQO1 demonstrated no selective toxicity toward BE-NQ cells or had no measurable cytotoxicity (IC<sub>50</sub> > 50 μM) (Table 6). Although compound **38** was a rather good substrate for NQO1, it displayed only minimal selective toxicity toward BE-NQ cells. This could be due to the less toxic nature of **38** (high IC<sub>50</sub> values for both cell lines) compared to other good substrates such as **30**, **33**, and **36** that have lower IC<sub>50</sub> values (Table 6). Overall, our results determined that the best lavendamycin substrates for NQO1 were also the most selectively toxic to the high NQO1 BE-NQ cell line.

**Molecular Modeling.** Computational and comparative molecular modeling studies were performed on two lavendamycin analogues, **31** and **37**, very poor and good substrates of NQO1, respectively. The molecular model-

**Table 7.** Number of Poses of Ligands **31** and **37** in Each Score Group of CSCORE Function

no.	<b>31</b>					<b>37</b>						
CSCORE	0	1	2	3	4	5	0	1	2	3	4	5
number of poses	18	8	-	-	4	-	3	3	1	4	15	4

ing was performed using SYBYL 6.9.1 software suite<sup>58</sup> (Tripos, Inc.; St. Louis, MO). Flexible docking was performed using the FlexX module of SYBYL that is capable of determining 30 possible conformations (poses) for each docked ligand.<sup>59,60</sup> Compound **65** (ARH019), 3-(hydroxymethyl)-5-(2-methylaziridin-1-yl)-1-methyl-2-phenylindole-4,7-dione,<sup>49</sup> has been suggested as an appropriate model for molecular docking studies of other compounds such as streptonigrin (**2**).<sup>25</sup> Therefore, the coordinates of the crystal structure of the human NQO1 complex with bound FAD and **65**, obtained from the Protein Data Bank (PDB ID code: 1H69<sup>25</sup>), were used as a composite reference structure for the docking experiments, wherein the coordinates of **65** served as the reference ligand of location. The docked conformations of ligands **31** and **37** were evaluated and ranked using FlexX and four scoring functions implemented in the CSCORE module in SYBYL. CSCORE is the consensus score computed from FlexX and ChemScore,<sup>61</sup> D-Score,<sup>62</sup> G-Score<sup>63</sup> and PMF-Score<sup>64</sup> scoring functions, in which docked poses are evaluated and ranked from 0 to 5; where 5 is the best fit to the model. Table 7 displays the number of conformations of ligands **31** and **37** in each score group of CSCORE function.

Ligand **37** possessed a higher number of poses with more optimal CSCORE values compared to **31** (Table 7). To minimize the number of false positives and/or negatives, visual screening of the binding orientations of the poses and geometric post-docking analyses were performed. The analyses included distance measurements, calculations, and pose geometries that determined (a) hydrogen-bonding interactions of the ligand poses with key residues of the NQO1 active site including Tyr-126, -128, and His-161, (b) hydride ion transfer

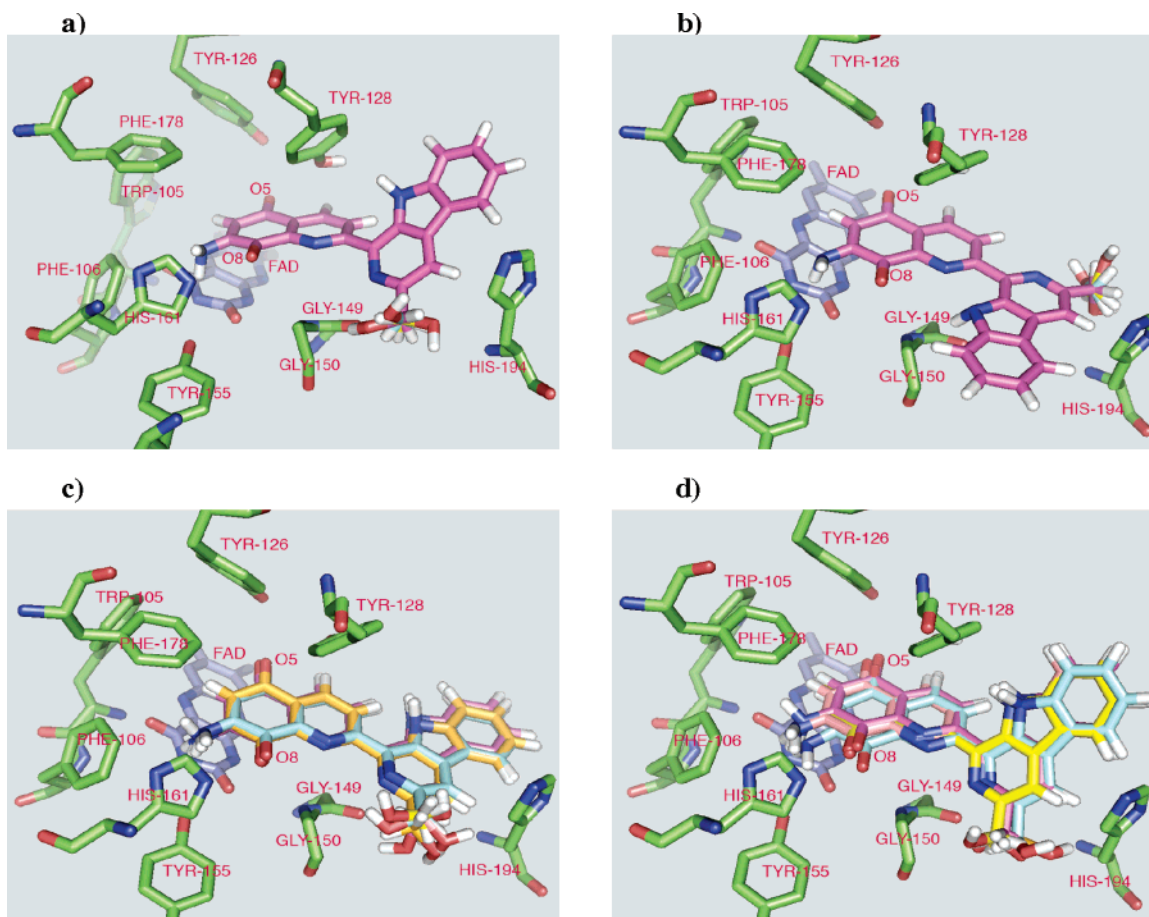


**Figure 2.** (a) View of the superposition of the docked poses 1,9 and 15 of **37** (magenta, cyan, and yellow) (CSCOREs = 5, 4, and 4) in NQO1 active site (RMSD = 0 Å). (b) View of the superposition of the docked poses 20, 24, and 27 of **37** (magenta, cyan, and yellow) (CSCOREs = 4) in NQO1 active site (RMSD = 0 Å). (c) View of the superposition of the docked poses 3, 4, 5, 6, 7, 11, and 12 of **37** (magenta, cyan, yellow, salmon, blue, orange and green) (CSCOREs = 4) in NQO1 active site (RMSD < 0.8 Å). (d) View of the superposition of the docked poses 8, 10, 18, 19, and 26 of **37** (yellow, salmon, magenta, cyan, and orange) (CSCOREs = 5, 5, 4, 4, and 4) in NQO1 active site (RMSD < 0.8 Å). Residues of the active site (lime), FAD (blue), and **37** represented as stick models. The atoms are colored: red, oxygen atoms; blue, nitrogen atoms; and white, hydrogen atoms.

from N5 of the FAD isoalloxazine ring to the ligands at either carbonyl oxygens (O5 or O8) or at a ring carbon, and (c) the angle between the quinone-moiety plane of the ligands and the FAD isoalloxazine ring (residue numbers in this paper are those used in the Protein Data Bank coordinates, PDB ID code: 1H69<sup>25</sup>).

Of the 30 possible docked conformations of ligand **37**, 24 poses (CSCORE  $\geq$  2) showed binding orientations similar to that of the reference ligand. Compound **65** has been shown to enter the active site by the 4,7-dione moiety where the plane of the indolequinone forms a partial aromatic-ring parallel stacking with the FAD isoalloxazine ring and the corresponding plane-to-plane angle is 16°. <sup>25</sup> The binding orientation of **65** and ligands **31** and **37** in the NQO1 active site were similarly determined by the atomic positioning of quinone carbonyl oxygens and atoms toward the isoalloxazine ring atoms of the FAD and residues of the active site. Compound **65** carbonyl oxygen O4 in comparison to O7 is positioned closer to Tyr-126, -128 and N5 of the FAD. <sup>25</sup> 19 poses of ligand **37** had CSCORE  $\geq$  4 (Table 7). Poses with CSCORE  $\geq$  4 fell into four clusters, where a cluster is defined as a group of poses that gives a root-mean-square (RMS) deviation less than 0.8 Å for the quinolinedione and indolopyridine moieties atoms. Poses 1, 9, and 15 (Figure 2a) and 20, 24, and 27 (Figure 2b)

fell into two clusters in which the RMS deviation of the poses equaled zero and the difference was in the binding orientation of the CH<sub>2</sub>OH group in NQO1 active site (Figures 2a and 2b). Poses 3, 4, 5, 6, 7, 11, and 12 (Figure 2c) and 8, 10, 18, 19, and 26 (Figure 2d) were clustered into two groups that yielded RMS deviations of < 0.8 Å. All of the clustered poses of **37** entered the active site by the 5,8-dione moiety similar to **65**, where the departure of the planes of most of these poses from a complete aromatic-ring parallel stacking with the FAD isoalloxazine ring closely resembled that of **65** (Figure 2). Carbonyl oxygen O5 of the clustered poses compared to O8 was positioned closer to Tyr-126, -128, and the FAD N5 resembling compound **65** binding orientation, suggesting that this could be the preferred binding orientation for ligand **37** (Figure 2).

In the NQO1 active site, the hydroxyl groups of Tyr-126 and -128 and/or N or NH of His-161 can form hydrogen bonds with carbonyl oxygens and/or other atoms of quinone substrates. <sup>10,25,27</sup> One crucial determining factor of quinone substrates binding strength in the NQO1 active site is the quinone oxygens' capability of forming hydrogen-bonding interactions with Tyr-126 and -128. <sup>27</sup> Good substrates for NQO1 such as **63** and **64** are capable of hydrogen-bonding interactions with the key residues of the NQO1 active site. <sup>6,25</sup> Among

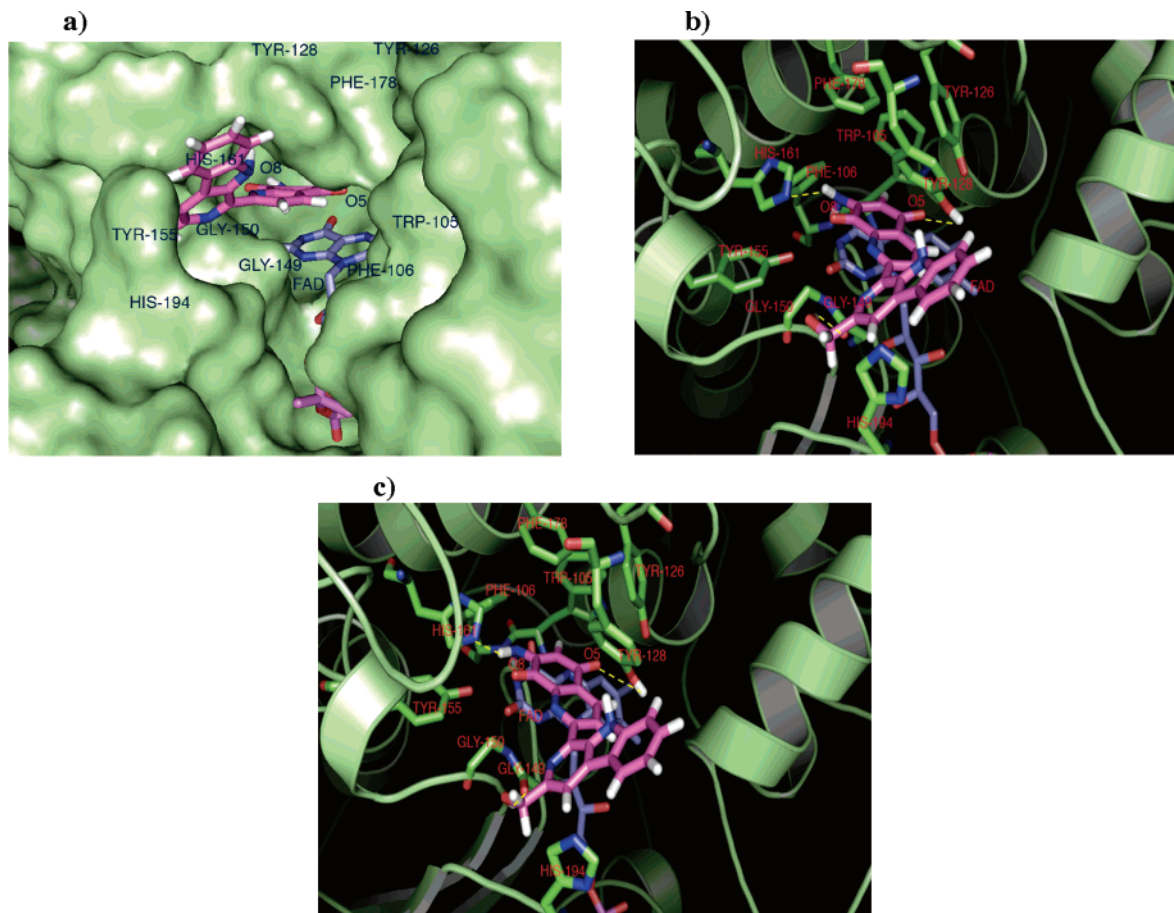


**Figure 3.** (a) Depiction of the molecular surface of NQO1 active site region. The surface of the pocket is colored lime with FAD (blue) and the docked pose 1 of **37** (magenta) (CSCORE = 5) represented as stick models. (b) Molecular model of the pose 1 of **37** docked into NQO1 active site. (c) Molecular model of the pose 2 of **37** (CSCORE = 5) docked into NQO1 active site. In b and c, residues of the active site (lime), FAD (blue), and **37** (magenta) represented as stick models and the rest of the structure as a secondary structure cartoon. The atoms are colored: red, oxygen atoms; blue, nitrogen atoms; and white, hydrogen atoms. Hydrogen bonds are represented as yellow dashed lines.

the poses of ligand **37**, poses 1 and 2 formed the highest number of efficient hydrogen bonds in the active site of the enzyme. The 5,8-dione moiety of pose 1 with CSCORE = 5 stacked over the isoalloxazine ring of the FAD and the NH<sub>2</sub> group at the quinolinedione 7-position was placed close to His 161 (Figures 3a and 3b). The fused three-ring indolopyridine moiety pointed toward the outside of the active site. The CH<sub>2</sub>OH group at the indolopyridine 2'-position was placed close to Gly-149 (Figures 3a and 3b). Pose 2 (CSCORE = 5) also positioned in the NQO1 active site in a very similar way to pose 1 (Figure 3c). The carbonyl oxygen O5 of ligand **37** poses 1 and 2 formed a hydrogen bond with the Tyr-128 OH and one hydrogen atom of the NH<sub>2</sub> substituent formed a hydrogen bond with N of His 161. The CH<sub>2</sub>-OH group of the indolopyridine moiety further stabilized the binding by making a hydrogen bond to the carbonyl oxygen of the Gly-149 (Figures 3b and 3c). Poses 1 and 2 of ligand **37** with high CSCOREs of 5 made the most efficient hydrogen-bonding interactions and had the most favorable binding orientation for efficient hydride ion reception and quinone reduction.

However, of the 30 possible docked conformations of ligand **31**, no conformation had a CSCORE = 5 (Table 7). None of the 30 poses had a binding orientation similar to that of the reference ligand, **65**. Pose 12 with CSCORE = 4 had a binding orientation opposite that

of the original reference (Figure 4a). Neither of the carbonyl oxygens O5 and O8 of pose 12 were capable of forming hydrogen bonds with the key residues of the active site unlike poses 1 and 2 of ligand **37** (Figure 4a). The other 3 poses (11, 26, and 28) of **31** with CSCORE = 4 entered the active site of NQO1 with the fused three-ring indolopyridine moiety where the quinolinedione moiety pointed toward the outside of the active site (Figures 4b and 4c). Compound **66** (ES1340), 5-methoxy-3-(phenyloxymethyl)-1,2-dimethylindole-4,7-dione,<sup>18</sup> which is a poor substrate for NQO1<sup>50</sup> has been shown to position in the NQO1 active site such that the 4,7-dione moiety points to the outside of the active site.<sup>26</sup> The binding orientations of the poses of ligand **31** were not favorable for effective hydrogen-bonding interactions, hydride ion reception, or quinone reduction. The remaining 26 poses with CSCOREs of 0 and 1 did not merit further considerations.

The molecular modeling and docking studies demonstrated that ligand **37** possessed an increased number of possible poses with favorable binding orientations to promote efficient hydrogen bonding interactions, hydride ion reception and quinone reduction compared to **31**. Ligand **37** due to the small hydrogen bond forming substituents possessed structural characteristics for favorable positioning in the NQO1 active site for reduction. Conversely, the unfavorable structural character-

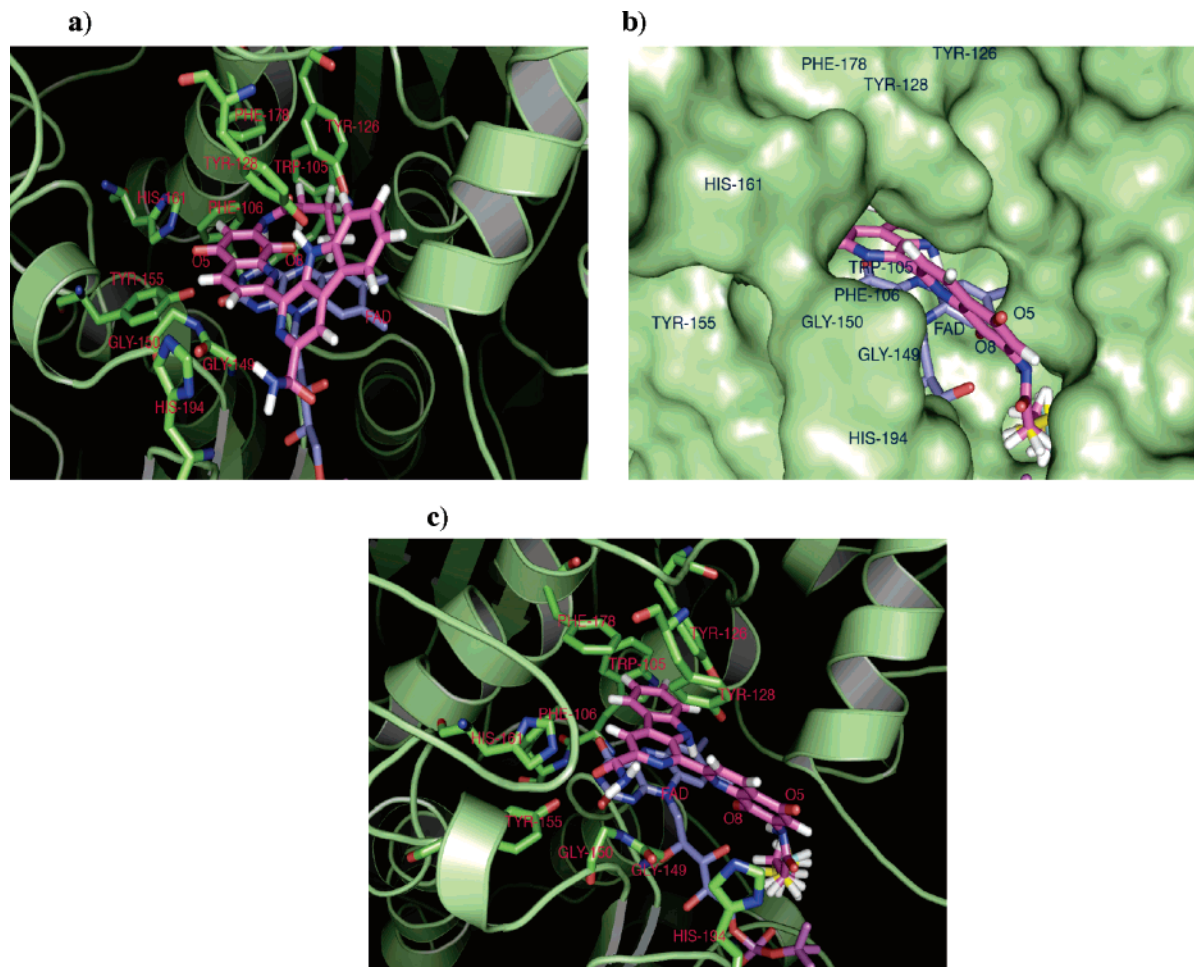


**Figure 4.** (a) Molecular model of the pose 12 of **31** (CSCORE = 4) docked into NQO1 active site. Residues of the active site (lime), FAD (blue), and **31** (magenta) represented as stick models and the rest of the structure as a secondary structure cartoon. (b) Depiction of the molecular surface of NQO1 active site region. The surface of the pocket is colored lime with FAD (blue) and the docked poses 11, 26, and 28 of **31** (magenta, yellow and cyan) (CSCOREs = 4) represented as stick models. (c) Molecular model of the poses 11, 26, and 28 of **31** docked into NQO1 active site. Residues of the active site (lime), FAD (blue), and **31** (magenta, yellow, and cyan) represented in stick models and the rest of the structure as a secondary structure cartoon. The atoms are colored: red, oxygen atoms; blue, nitrogen atoms; and white, hydrogen atoms.

istics of ligand **31** could exclude it from proper positioning in the NQO1 active site for reduction. These findings suggest that active site positioning contributes to the much greater substrate specificity observed for ligand **37** than ligand **31**.

**Conclusions.** A number of novel lavendamycin analogues were synthesized through short and practical methods. No direct correlation between the reduction potential and rate of reduction of the analogues by NQO1 were found suggesting the more important role of steric effects of these compounds in the NQO1 active site rather than electronic effects on the reduction efficiency by NQO1. Small substituents at R<sup>1</sup> and R<sup>3</sup> positions on the quinonolinedione moiety of the lavendamycin analogues were well tolerated whereas absence of a substituent at R<sup>2</sup> was preferred. Addition of NH<sub>2</sub> and CH<sub>2</sub>OH groups at R<sup>1</sup> and R<sup>3</sup> positions, respectively, displayed the greatest positive impact on substrate specificity such that 2'-CH<sub>2</sub>OH-7-NH<sub>2</sub> derivative (**37**) exhibited the highest reduction rate. The best lavendamycin substrates for NQO1 were also the most selectively toxic to the NQO1-rich BE-NQ cell line. The docking studies supported a model in which the good lavendamycin substrate **37** was capable of efficient

hydrogen-bonding interactions with the key residues of the NQO1 active site and hydride ion reception from FAD while the poor substrate **31** was not. The use of molecular modeling techniques can greatly contribute to future rational design of good NQO1 substrates for NQO1-directed lavendamycin antitumor agent development.

## Experimental Section

**Chemistry. General Methods.** For General Methods see ref 38 (*J. Med. Chem.* **2003**, *46*, 5773–5780). Aziridine was prepared according to the procedure previously described by Allen et al.<sup>65</sup> and was kept in a refrigerator over KOH pellets.

**Bis(chloroacetamido)-8-hydroxy-2-methylquinoline (50).** In a 500 mL heavy-walled hydrogenation bottle, 5.25 g (0.21 mol) of finely ground 8-hydroxy-2-methyl-5,7-dinitroquinoline (**47**) and 1.75 g of palladium on charcoal were suspended in a mixture of 90 mL of water and 9 mL of concentrated hydrochloric acid.<sup>41</sup> In a Parr Hydrogenator, this mixture was shaken under 30 psi of hydrogen for 20 h. The catalyst was filtered off, and the dark red solution containing the dihydrochloride salt of 5,7-diamino-8-hydroxy-2-methylquinoline was placed in a 250 mL round-bottomed flask with a magnetic bar. To this stirred solution was added in sequence as quickly as possible 12 g of sodium sulfite, 16 g of sodium acetate, and 65 g of chloroacetic anhydride. Heat was evolved with formation

of a light colored precipitate which was dissolved after 15 min. The solution gave a precipitate after stirring for 1 h. This mixture was poured into 100 mL of ice-water mixture and stirred for 5 min and then filtered. The product was washed with 10 mL of cold ethanol and filtered. The filtrate upon standing overnight gave more of the product. The total weight of the product was 3.61 g (50%). It was recrystallized from ethanol-water: mp 194–196 °C;  $^1\text{H NMR}$  (DMSO- $d_6$ )  $\delta$  2.71 (s, 3H), 4.37 (s, 2H), 4.44 (s, 2H), 7.43 (d, 1H,  $J = 8.8$ ), 8.15 (d, 1H,  $J = 8.8$ ), 8.16 (s, 1H), 9.89 (br s, 1H), 10.18 (br s, 1H); EIMS,  $m/z$ , 341/343 ( $M^+$  1.5/1, 52), 305 (60), 292 (base), 264 (28), 228 (60), 188 (70), 160 (17); HRMS calculated for  $\text{C}_{14}\text{H}_{13}\text{Cl}_2\text{N}_3\text{O}_3$  341.033397, found 341.033888; Elemental analysis: calculated for C, 49.14; H, 3.83; Cl, 20.72; N, 12.28, found C, 49.24; H, 3.89; Cl, 20.43; N, 12.6.

#### 7-Chloroacetamido-2-methylquinoline-5,8-dione (41).

In a 500 mL round-bottomed flask, equipped with a magnetic bar, 5,7-bis(chloroacetamido)-8-hydroxy-2-methylquinoline (3.42 g, 0.01 mol) was suspended in 122 mL of glacial acetic acid. To this, a solution of potassium dichromate (8.8 g, 0.03 mol) in 115 mL of water was added and stirred overnight at room temperature. The solution was extracted with dichloromethane (12  $\times$  50 mL). The organic extracts were washed with 200 mL of sodium bicarbonate solution, dried with magnesium sulfate, and then evaporated under reduced pressure to give a bright yellow solid (1.56 g, 59%). Recrystallization from ethyl acetate gave the pure product: mp 196–200 °C (dec);  $^1\text{H NMR}$  ( $\text{CDCl}_3$ )  $\delta$  2.76 (s, 3H), 4.23 (s, 2H), 7.56 (d, 1H,  $J = 8.1$ ), 7.89 (s, 1H), 8.30 (d, 1H,  $J = 8.1$ ), 9.48 (br s, 1H); EIMS,  $m/z$ , 264/266 ( $M^+$  2.9/1), 229 (62), 215 (74), 201 (43), 188 (86), 161 (base), 132 (21); HRMS calculated for  $\text{C}_{14}\text{H}_9\text{ClN}_2\text{O}_3$  264.03107 found 264.029824; Elemental analysis calculated for C, 54.19; H, 3.43; Cl, 13.40; N, 10.58, found C, 54.19; H, 3.37; Cl, 13.29; N, 10.36.

#### 7-Chloroacetamido-2-formyl-5,8-quinolinedione (4).

In a 25 mL round-bottomed flask, equipped with a magnetic bar, water-cooled reflux condenser, and argon-filled balloon, dione **41** (0.529 g, 2 mmol), selenium dioxide (0.332 g, 3 mmol), 12 mL of dried distilled dioxane, and 0.25 mL of water were stirred and slowly heated to reflux over a 2 h period. To complete the reaction, the mixture was refluxed for 17 h (TLC). An additional 10 mL of dioxane was added and refluxed for 10 min and then filtered off hot. The filter cake was placed in a round-bottomed flask, and 10 mL of dichloromethane was added and refluxed for 10 min and then filtered. The filtrates were combined and then evaporated to dryness under reduced pressure. The solid residue was dissolved in 50 mL of dichloromethane, placed in a separatory funnel, and washed with 3% sodium bicarbonate solution. The aqueous layers were extracted with 3  $\times$  50 mL of dichloromethane and the combined organic layers were dried ( $\text{MgSO}_4$ ) and evaporated to give 0.25 g (45%) of a yellow product: mp 190–192 °C;  $^1\text{H NMR}$  ( $\text{CDCl}_3$ )  $\delta$  4.26 (s, 2H), 8.04 (s, 1H), 8.33 (d, 1H,  $J = 8.1$ ), 8.62 (d, 1H,  $J = 8.1$ ), 9.54 (br s, 1H), 10.28 (s, 1H); EIMS,  $m/z$ , 278/280 ( $M^+$  2.7/1, 95), 243 (33), 229 (33), 215 (55), 202 (base), 175 (61); HRMS calculated for  $\text{C}_{14}\text{H}_9\text{ClN}_2\text{O}_3$  278.009435, found 278.00876.

**Tryptophan *n*-Pentyl Ester (8).** This ester was prepared according to the method used for the preparation of **9** in 80% yield as a thick yellow oil.  $^1\text{H NMR}$  ( $\text{CDCl}_3$ )  $\delta$  0.89 (t, 3H,  $J = 6.6$ ), 1.1–1.3 (m, 2H), 1.4–1.7 (m, 4H), 2.9–3.7 (m, 2H), 3.70–3.80 (m, 1H), 4.02 (t, 2H,  $J = 6.7$ ), 6.98 (s, 1H), 7.01–7.2 (m, 2H), 7.22 (d, 1H,  $J = 7.6$ ), 7.56 (d, 1H,  $J = 7.6$ ), 8.14 (br s, 1H); HRMS calculated for  $\text{C}_{16}\text{H}_{22}\text{N}_2\text{O}_2$  ( $M^+$ ) 274.1676, found 274.1678.

**Tryptophan Isoamyl Ester (9).** Isoamyl alcohol was dried over anhydrous cupric sulfate for 24 h and then distilled under argon. Tryptophan (1.43 g, 7 mmol) was placed in a 100 mL round-bottomed flask along with 60 mL of the dried isoamyl alcohol and 10 mL of HCl/ether solution. The solution was refluxed in an oil bath for 22 h. The mixture was then rotaevaporated to dryness. A portion of the resulting tryptophan isoamyl ester hydrochloride (723 mg, 2.84 mmol) was suspended in 36 mL of ethyl acetate. To this stirred suspen-

sion, a 14% solution of ammonium hydroxide (~3 mL) was added until the aqueous layer was at pH = 8. The aqueous layer was separated, and the organic layer was washed with a saturated sodium chloride solution (3  $\times$  2 mL) and water (2 mL) and dried over magnesium sulfate. The solution was filtered and rotaevaporated to dryness. The thick liquid was further dried under a vacuum pump at 50–60 °C for 2 days. The total weight of the product was 1.6 g (83%): mp 50 °C (Dec.);  $^1\text{H NMR}$  ( $\text{CDCl}_3$ )  $\delta$  0.90 (d, 6H,  $J = 6.3$ ), 1.60 (m, 4H), 2.99–3.22 (m, 2H), 3.81 (m, 1H), 4.10 (t, 2H,  $J = 6.7$ ), 7.00 (s, 1H), 7.10 (m, 1H), 7.20 (m, 1H), 7.33 (d, 1H,  $J = 7.6$ ), 7.59 (d, 1H,  $J = 7.3$ ), 8.08 (br s, 1H); HRMS calculated. For  $\text{C}_{16}\text{H}_{22}\text{N}_2\text{O}_2$  ( $M^+$ ) 274.1676, found 274.1676.

**Tryptophan *n*-Hexyl Ester (10).** Ester **10** was prepared by a similar method as that for ester **9** in 87% yield as thick oil.  $^1\text{H NMR}$  ( $\text{CDCl}_3$ )  $\delta$  0.89 (t, 3H,  $J = 7.0$ ), 1.20–1.40 (m, 4H), 1.50–1.75 (m, 4H), 2.90–3.40 (m, 2H), 3.78–3.90 (m, 1H), 4.1 (t, 2H,  $J = 7.0$ ), 7.09 (s, 1H), 7.16–7.25 (m, 2H), 7.37 (d, 1H,  $J = 8.0$ ), 7.64 (d, 1H,  $J = 6.6$ ), 8.12 (br s, 1H); HRMS calculated for  $\text{C}_{17}\text{H}_{24}\text{N}_2\text{O}_2$  ( $M^+$ ) 288.1832, found 288.1824.

#### *N*-Carbobenzyloxytryptophan Succinimide Ester (60).

In a 100 mL round-bottomed flask equipped with a magnetic bar and an argon-filled balloon, *N*-carbobenzyloxytryptophan (2.132 g, 6.3 mmol), *N*-hydroxysuccinimide (0.725 g, 6.3 mmol), and 50 mL dried, distilled dioxane were placed. The reaction mixture was stirred until a clear solution was obtained, the flask was kept in a cold-water bath at 12 °C (dioxane freezes at 11 °C), and *N*-dicyclohexylcarbodiimide (1.3 g, 6.3 mmol) was added. A white precipitate was immediately formed. The mixture was stirred at 15–20 °C for 2 h and then at room temperature for another 2 h. The mixture was allowed to stand in refrigerator overnight and then filtered. The solid was washed with dioxane (2  $\times$  3 mL). The filtrate was rotaevaporated to a thick liquid and then kept on a vacuum pump for 3 days to give a white solid. The total weight of the product was 3.19 g (>100%). Some dioxane (shown by NMR) was still present in the product that was taken into consideration when **59** was used in the following reactions. An analytical sample was obtained by silica gel plate chromatography using EtOAc–acetone–MeOH (1:1:0.5) as the eluant. The yield of the pure product was 89%; mp 64 °C;  $^1\text{H NMR}$  ( $\text{CDCl}_3$ )  $\delta$  2.73 (s, 4H), 3.42–3.50 (m, 2H), 5.07–5.17 (m, 3H), 7.07 (dd, 1H,  $J = 7.0$ ), 7.07–7.14 (m, 1H), 7.13 (dd, 1H,  $J = 8.0$ ), 7.17 (s, 1H), 7.34 (s, 5H), 7.54 (d, 1H,  $J = 7.4$ ), 8.27 (br s, 1H); HRMS calculated for  $\text{C}_{25}\text{H}_{21}\text{N}_3\text{O}_6$  435.1430, found 435.1428.

#### *N*-Carbobenzyloxytryptophan Piperidine Amide (61).

In a 50 mL round-bottomed two-necked flask equipped with a magnetic bar and an argon-filled balloon, ester **60** (0.435 g, 1 mmol), piperidine (0.085 g, 1 mmol), dried distilled triethylamine (0.14 mL, 1.4 mmol), absolute ethanol (13 mL), and distilled chloroform (12 mL) were placed. The reaction mixture was stirred for 1 h at room temperature. Thin-layer chromatography showed the reaction to be completed. The mixture was evaporated under reduced pressure to give a solid. The material was dissolved in 90 mL of ethyl acetate and then washed with 30 mL of water followed by 2  $\times$  30 mL of 10% citric acid. The solution was washed with 15 mL 1 N sodium bicarbonate, then 5 mL of water, dried ( $\text{Na}_2\text{SO}_4$ ), and evaporated to give a white solid. The product was dried on a vacuum pump at 60 °C for 2 days yielding 0.32 g (80%) of the product **61**: mp 64–64.5 °C;  $^1\text{H NMR}$  ( $\text{CDCl}_3$ )  $\delta$  0.76–1.40 (m, 6H), 2.85–3.39 (m, 4H), 3.38–3.40 (m, 2H), 4.99–5.05 (m, 1H), 5.11 (s, 2H), 5.88 (s, 1H), 6.98 (s, 1H), 7.13 (t, 1H,  $J = 7.7$ ), 7.17 (t, 1H,  $J = 6.7$ ), 7.18 (d, 1H,  $J = 6.7$ ), 7.34 (s, 5H), 7.62 (d, 1H,  $J = 7.7$ ), 8.22 (br s, 1H); HRMS calculated for  $\text{C}_{24}\text{H}_{27}\text{N}_3\text{O}_3$  405.2047, found 405.2048.

**Tryptophan Piperidine Amide (11).** In a 50 mL two-necked round-bottomed flask equipped with a magnetic bar and an argon-filled balloon, amide **61** (0.65 g, 1.6 mmol) was suspended in 30 mL of distilled methanol. To this mixture dry ammonium formate (0.298 g, 4.73 mmol) and 0.298 g of 10% Pd/C were added and stirred at room temperature. Thin-layer chromatography showed the completion of the reaction in 30 min. The mixture was filtered and Pd/C was rinsed with 10

mL of methanol. The filtrate was evaporated under reduced pressure until a thick liquid with consistency and color of honey was obtained. The thick liquid was dried on a vacuum pump at 50–60 °C for 2 days. The product weighed 0.224 g, (70%): mp 172–173 °C;  $^1\text{H NMR}$  ( $\text{CDCl}_3$ )  $\delta$  0.77–1.37 (m, 6H), 2.88–3.37 (m, 4H), 4.12 (t, 1H,  $J = 6.6$ ), 4.73 (br s, 2H), 6.98 (d, 1H,  $J = 8.0$ ), 7.03 (dd, 1H,  $J = 8.7$ , 7.6), 7.16 (s, 1H), 7.33 (d, 1H,  $J = 8.0$ ), 7.48 (d, 1H,  $J = 7.7$ ); HRMS calculated for  $\text{C}_{16}\text{H}_{22}\text{N}_3\text{O}$  ( $\text{M} + \text{H}$ ) $^+$  272.1762, found 272.1754.

***N*-Carbobenzyloxytryptophan Morpholine Amide (62).** The procedure for the preparation of **62** was the same as that for **61** yielding 0.37 g (90%) of the honey-colored product: mp 71.5–72 °C;  $^1\text{H NMR}$  ( $\text{CDCl}_3$ )  $\delta$  2.37–2.83 (m, 2H), 3.08–3.54 (m, 8H), 4.95–5.01 (m, 1H), 5.12 (s, 2H), 5.82 (br s, 1H), 7.04 (s, 1H), 7.08–7.23 (m, 3H), 7.35 (s, 5H), 7.65 (d, 1H,  $J = 7.2$ ), 8.10 (br s, 1H); HRMS calculated for  $\text{C}_{23}\text{H}_{25}\text{N}_3\text{O}_4$  407.1840, found 407.1846.

**Tryptophan Morpholine Amide (12).** The procedure for the preparation of **12** was the same as that for **11** to give the product in 88% yield: mp 99–101 °C;  $^1\text{H NMR}$  ( $\text{CDCl}_3$ )  $\delta$  1.82 (br s, 2H), 2.68–3.49 (m, 2H), 2.98–3.44 (m, 8H), 4.08 (t, 1H,  $J = 7.2$ ), 7.09 (s, 1H), 7.17–7.21 (m, 2H), 7.58 (d, 1H,  $J = 7.0$ ), 8.13 (br s, 1H); HRMS calculated for  $\text{C}_{15}\text{H}_{22}\text{N}_3\text{O}_2$  ( $\text{M} + \text{H}$ ) $^+$  273.1477, found 273.1476.

**General Procedure for the Synthesis of Lavendamycins.** Unless otherwise stated, lavendamyacin derivatives **14**–**23** were synthesized by the procedure described for analogue **16**. For each compound, the corresponding starting materials (Scheme 1) were mixed in the desired solvent and heated for several hours (Table 1). The completion of each reaction was monitored by TLC. Using a similar setup to that of **16**, lavendamycins **32**, **39**, **57**, and **58** were also synthesized as described in the text.

**7-*N*-Acetyldecarboxydemethylavendamyacin (14).** A mixture of aldehyde **3** (70 mg, 0.29 mmol) and tryptamine **5** (50 mg, 0.31 mmol) in 180 mL of dry anisole was heated to 105 °C over a period of 2 h and then 10% Pd/C (70 mg) was added and refluxed for 17 h. The reaction mixture was filtered while hot, and the solid was washed with chloroform and then acetone. Rotaevaporation of the filtrate gave **14** as a yellow solid (91.6 mg, 83%): mp > 280 °C;  $R_f = 0.42$  ( $\text{Al}_2\text{O}_3$ , 0.03/100 MeOH/ $\text{CH}_2\text{Cl}_2$ );  $^1\text{H NMR}$  ( $\text{CDCl}_3$ )  $\delta$  2.37 (s, 3H), 7.30–7.40 (m, 1H), 7.62–7.71 (m, 1H), 7.74 (d, 1H,  $J = 8.0$ ), 7.99 (s, 1H), 8.13 (d, 1H,  $J = 4.8$ ), 8.21, d, 1H,  $J = 8.0$ ), 8.45 (br s, 1H), 8.54 (d, 1H,  $J = 8.0$ ), 8.61 (d, 1H,  $J = 4.8$ ), 9.10 (d, 1H,  $J = 8.0$ ), 11.64 (br s, 1H); HRMS calculated for  $\text{C}_{22}\text{H}_{14}\text{N}_4\text{O}_3$  ( $\text{M}^+$ ) 382.1066, found 382.1069.

**7-*N*-Acetyldeethylavendamyacin Methyl Ester (15).** Analogue **15** was prepared according to the method used for **16**. A mixture of 0.3 mmol of each of **3** and **6** in 180 mL of dry anisole was heated (see Table 1 for temperature and time). The reaction mixture was evaporated to give a light yellow solid. The solid was washed with acetone to give 64 mg of a pure yellow product. More product (34 mg) was obtained from the filtrate (total yield, 67%): mp > 280 °C;  $R_f = 0.41$  (0.01/20 MeOH/ $\text{CH}_2\text{Cl}_2$ );  $^1\text{H NMR}$  ( $\text{CDCl}_3$ )  $\delta$  2.38 (s, 3H), 4.12 (3, 3H), 7.40 (unresolved dd, 1H,  $J = 7.6$ ), 7.76 (unresolved dd, 1H,  $J = 7.6$ ), 8.03 (m, 1H), 8.27 (d, 1H,  $J = 8.2$ ), 8.48 (br s, 1H), 8.62 (d, 1H,  $J = 8.2$ ), 9.03 (s, 1H), 9.26 (d, 1H,  $J = 8.2$ ), 11.82 (br s, 1H); HRMS calculated for  $\text{C}_{24}\text{H}_{16}\text{N}_4\text{O}_5$  ( $\text{M}^+$ ) 440.1120, found 440.1119.

**7-*N*-Acetyldeethylavendamyacin *n*-Butyl Ester (16).** In a 500 mL three-necked round-bottomed flask equipped with a Dean–Stark trap, a magnetic bar, and under an argon flow, 7-acetamido-2-formylquinoline-5,8-dione (**3**, 133 mg, 0.51 mmol) and tryptophan butyl ester (**7**, 124 mg, 0.52 mmol) were dissolved in 162 mL of dry xylene and, while being stirred, heated to reflux over a 3-h period. The yellow lemon solution was refluxed for 5 h and evaporated in vacuo, and the residue was dissolved in chloroform. The small amount of the brownish solid was removed, and the solution was concentrated to near dryness. Acetone, 2 mL, was added and the resulting solid material was filtered, washed with a small portion of acetone, and dried under vacuum. The orange solid weighed 155 mg

(63%): mp 256–257 °C;  $R_f = 0.74$  (1/100 MeOH/ $\text{CH}_2\text{Cl}_2$ );  $^1\text{H NMR}$  ( $\text{CDCl}_3$ )  $\delta$  1.05 (t, 3H,  $J = 7.0$ ), 1.5–1.62 (m, 2H), 1.84–1.94 (m, 2H), 2.36 (s, 3H), 4.51 (t, 2H,  $J = 7.0$ ), 7.4 (unresolved dd, 1H,  $J, J' \approx 7.3$ , 1H), 7.64–7.70 (m, 1H), 7.72 (d, 1H,  $J = 8.1$ ), 7.97 (s, 1H), 8.24 (d, 1H,  $J = 8.1$ ), 8.4 (br s, 1H), 8.53 (d, 1H,  $J = 8.4$ ), 8.94 (s, 1H), 9.17 (d, 1H,  $J = 8.4$ ), 11.77 (br s, 1H); HRMS (FAB) calculated for  $\text{C}_{27}\text{H}_{25}\text{N}_4\text{O}_5$  ( $\text{M} + 3\text{H}$ ) $^+$  485.1825, found 485.1827.

**7-*N*-Acetyldeethylavendamyacin *n*-Pentyl Ester (17).** Analogue **17** was synthesized according to the procedure used for **16** in 44% yield as an orange solid: mp 232–233 °C;  $R_f = 0.68$  (1/100 MeOH/ $\text{CH}_2\text{Cl}_2$ );  $^1\text{H NMR}$  ( $\text{CDCl}_3$ )  $\delta$  0.99 (t, 3H,  $J = 6.9$ ), 1.40–1.80 (m, 4H), 1.8–2.0 (m, 2H), 2.35 (s, 3H), 4.48 (t, 2H,  $J = 6.6$ ), 7.30–7.40 (m, 1H), 7.50–7.65 (m, 2H), 7.86 (s, 1H), 8.17 (d, 1H,  $J = 8.0$ ), 8.29 (br s, 1H), 8.36 (d, 1H,  $J = 8.4$ ), 8.89 (s, 1H), 9.02 (d, 1H,  $J = 8.4$ ), 11.56 (br s, 1H); HRMS (FAB) calculated for  $\text{C}_{28}\text{H}_{27}\text{N}_4\text{O}_5$  ( $\text{M} + 3\text{H}$ ) $^+$  499.1981, found 499.1980.

**7-*N*-Acetyldeethylavendamyacin Isoamyl Ester (18).** Compound **18** was prepared according to the method similar to that of **16**. A mixture of 0.5 mmol of each of the starting materials **3** and **9** in 160 mL of dry xylene was heated to 78 °C over a period of 4 h and then heated to 125 °C over 10 min and kept at 125–130 °C for 5.5 h. The reaction mixture was allowed to cool to room temperature, and the brown solid impurity was filtered. The filtrate containing the product was concentrated to near dryness and then washed with a small amount of acetone to give 84 mg of an orange yellow solid. More product was obtained from the concentration of the filtrate (total yield, 128 mg, 50%): mp 257.5–258 °C;  $R_f = 0.64$  (1/100 MeOH/ $\text{CH}_2\text{Cl}_2$ );  $^1\text{H NMR}$  ( $\text{CDCl}_3$ )  $\delta$  1.06 (d, 6H,  $J = 6.3$ ), 1.8–1.9 (m, 3H), 2.38 (s, 3H), 4.54 (t, 2H,  $J = 6.8$ ), 7.35–7.45 (m, 1H), 7.63–7.80 (m, 2H), 8.01 (s, 1H), 8.27 (d, 1H,  $J = 7.7$ ), 8.45 (br s, 1H), 8.58 (d, 1H,  $J = 8.3$ ), 8.97 (s, 1H), 9.22 (d, 1H,  $J = 8.3$ ), 11.80 (br s, 1H); HRMS calculated for  $\text{C}_{28}\text{H}_{24}\text{N}_4\text{O}_5$  ( $\text{M}^+$ ) 496.1760, found 496.1756.

**7-*N*-Acetyldeethylavendamyacin *n*-Hexyl Ester (19).** This compound was synthesized using the method for the preparation of **16**. The orange solid was obtained in 54% yield: mp 228–230 °C;  $R_f = 0.51$  (1/100 MeOH/ $\text{CH}_2\text{Cl}_2$ );  $^1\text{H NMR}$  ( $\text{CDCl}_3$ )  $\delta$  0.94 (t, 3H,  $J = 7.0$ ), 1.36–1.50 (m, 4H), 1.50–1.60 (m, 2H), 1.80–2.0 (m, 2H), 4.48 (t, 2H,  $J = 6.8$ ), 7.30–7.42 (m, 1H), 7.60–7.70 (m, 2H), 7.90 (s, 1H), 8.16 (d, 1H,  $J = 8.0$ ), 8.33 (s, 1H), 8.60 (d, 1H,  $J = 8.4$ ), 8.87 (s, 1H), 9.07 (d, 1H,  $J = 8.4$ ), 11.64 (s, 1H); HRMS calculated for  $\text{C}_{29}\text{H}_{26}\text{N}_4\text{O}_5$  ( $\text{M} + 3\text{H}$ ) $^+$  513.2138, found 513.2139.

**7-*N*-Acetyldeethylavendamyacin Piperidine Amide (20).** In a method similar to that used for the preparation of **16**, a mixture of 0.55 mmol of aldehyde **3** in 300 mL of dry anisole was heated to 70 °C, and then in a dropping funnel, a solution of 0.55 mmol of tryptophan piperidine amide in 6 mL of dry pyridine was dropwise added and heated for the required amount time (Table 1). The reaction mixture was cooled to room temperature, and the solid was filtered, washed with 10 mL of dichloromethane followed by 25 mL of ethyl acetate, and then vacuum-dried to yield 120 mg of a brown product. The filtrate was evaporated, and from the solid residue more product (34 mg) was recovered through flash chromatography using chloroform as the eluting solvent (total yield, 56%): mp 250 °C (dec);  $R_f = 0.39$  (0.01/5 MeOH/ $\text{CH}_2\text{Cl}_2$ );  $^1\text{H NMR}$  ( $\text{CDCl}_3$ )  $\delta$  1.70–1.77 (m, 6H), 2.43 (s, 3H), 3.71–3.89 (m, 4H), 7.28–7.32 (m, 1H), 7.59–7.61 (m, 2H), 7.99 (s, 1H), 8.09 (d, 1H,  $J = 8.4$ ), 8.32 (d, 1H,  $J = 8.4$ ), 8.41 (s, 1H), 8.92 (d, 1H,  $J = 8.4$ ), 11.44 (br s, 1H); HRMS calculated for  $\text{C}_{28}\text{H}_{24}\text{N}_5\text{O}_4$  ( $\text{M} + \text{H}$ ) $^+$  494.1828, found 494.1834.

**7-*N*-Acetyldeethylavendamyacin Morpholine Amide (21).** In a method similar to that used for the synthesis of **16**, compound **21** was synthesized according to the method used for **20** as an orange solid in a total yield of 57%: mp > 300 °C;  $R_f = 0.38$  (0.03/5 MeOH/ $\text{CH}_2\text{Cl}_2$ );  $^1\text{H NMR}$  ( $\text{CDCl}_3$ )  $\delta$  2.40 (s, 3H), 3.79–3.96 (m, 8H), 7.38–7.41 (m, 1H), 7.65–7.8 (m, 2H), 8.03 (s, 1H), 8.20 (d, 1H,  $J = 8.1$ ), 8.5–8.65 (m, 3H), 8.97 (d, 1H,  $J = 8.3$ ), 11.67 (br s, 1H); HRMS calculated for  $\text{C}_{27}\text{H}_{24}\text{N}_5\text{O}_5$  ( $\text{M} + 3\text{H}$ ) $^+$  498.1777, found 498.1781.

**7-N-Acetyldecarydemethyl-2'-(hydroxymethyl)-lavendamyacin (22).** Compound **22** was prepared by the condensation of 0.15 mmol of **3** and 0.15 mmol of **13** in 60 mL of anisole. The mixture was heated to 155 °C over a period of 4 h and then allowed to cool to room temperature. The yellow solid product was filtered, washed with acetone, and dried under vacuum (29.4 mg, 48%): mp > 280 °C;  $R_f = 0.39$  (EtOAc);  $^1\text{H NMR}$  ( $\text{CDCl}_3$ )  $\delta$  2.31 (s, 3H), 4.88 (d, 1H,  $J = 5.9$ ), 5.58 (t, 1H,  $J = 5.9$ ), 7.33–7.38 (m, 1H), 7.63–7.71 (m, 2H), 7.82 (s, 1H), 8.41 (d, 1H,  $J = 7.7$ ), 8.54 (d, 1H,  $J = 8.0$ ), 8.96 (d, 1H,  $J = 8.0$ ), 10.29 (br s, 1H), 11.67 (br s, 1H); HRMS calculated for  $\text{C}_{23}\text{H}_{16}\text{N}_4\text{O}_4$  ( $\text{M}^+$ ) 412.1171, found 412.1175.

**7-N-Chloroacetyldemethyllavendamyacin Isoamyl Ester (23).** A mixture of 0.18 mmol of **4** and 0.18 mmol of **9** in 75 mL of dry xylene was heated slowly to 76 °C over 5 h. The mixture was filtered hot to remove the impurity, and the filtrate was concentrated under reduced pressure to about 10 mL. The solution was kept in a refrigerator overnight to give a dark orange-brown solid. The solid was filtered and washed with cold ethyl acetate yielding 25 mg of the product. Further concentration of the filtrate afforded more product (total 40.5 mg, 43%): mp 280–284 °C;  $R_f = 0.40$  (0.008/5 MeOH/ $\text{CHCl}_3$ );  $^1\text{H NMR}$  ( $\text{CDCl}_3$ )  $\delta$  1.05 (d, 6H,  $J = 6.3$ ), 1.76–1.95 (m, 3H), 4.29 (s, 2H), 4.52 (t, 2H,  $J = 6.8$ ), 7.39 (unresolved dd, 1H,  $J = 8.0$ ), 7.78 (d, 1H,  $J = 8.0$ ), 7.95 (s, 1H), 8.23 (d, 1H,  $J = 8.0$ ), 8.54 (d, 1H,  $J = 8.3$ ), 8.93 (s, 1H), 9.18 (d, 1H,  $J = 8.3$ ), 9.56 (s, 1H), 11.76 (br s, 1H); HRMS calculated for  $\text{C}_{28}\text{H}_{23}\text{ClN}_4\text{O}_5$  530.1357, found 530.1358.

**7-N-Acetyl-6-pyrrolidinolavendamyacin Methyl Ester (24).** To a stirred solution of 7-acetyllavendamyacin methyl ester<sup>41,42</sup> (**3**, 50 mg, 0.11 mmol) in dry chloroform (30 mL) was added pyrrolidine (0.2 mL, 170 mg, 2.4 mmol), and the resulting red-brown solution was allowed to stir at room temperature for 2 h. The reaction mixture was rotaevaporated to dryness. The solid was washed with ether (10 mL) and dried under vacuum pump to afford 51 mg (88%) of the product as a reddish brown powder: mp 210 °C (dec);  $R_f = 0.13$  (Et OAc/ $\text{CH}_2\text{Cl}_2$  1/1);  $^1\text{H NMR}$  ( $\text{DMSO}-d_6$ )  $\delta$  1.75–1.96 (br m, 4H), 2.11 (s, 3H), 3.11 (3H, s), 3.11 (s, 3H), 3.78–3.58 (br m, 4H), 3.98 (s, 3H), 7.48–7.41 (m, 1H), 7.70–7.76 (m, 1H), 7.82 (d, 1H,  $J = 7.9$ ), 8.45 (d, 1H,  $J = 7.9$ ), 8.50 (d, 1H,  $J = 8.2$ ), 8.78 (d, 1H,  $J = 8.2$ ), 9.33 (s, 1H), 12.36 (s, 1H); EAB–HRMS calculated for  $\text{C}_{29}\text{H}_{25}\text{N}_5\text{O}_5\text{Na}$  ( $\text{M} + \text{Na}^+$ ) 546.1753, found 546.1779.

**7-N-Acetyl-6-aziridinodemethyllavendamyacin Amide (25).** To a stirred solution of 7-acetyldemethyllavendamyacin amide<sup>38</sup> (**5**, 50 mg, 0.12 mmol) in dry chloroform (25 mL) and dry ethanol (25 mL) was added aziridine (0.7 mL, 58 mg, 13.5 mmol), and the resulting reddish brown solution was allowed to stir at room temperature for 48 h. Then the reaction mixture was rotaevaporated to dryness. The solid was washed with ether (10 mL) and further dried under a vacuum pump to afford 52 mg (93%) of the product as a reddish brown powder: mp > 260 °C;  $R_f = 0.88$  (MeOH/ $\text{CH}_2\text{Cl}_2$  1/10);  $^1\text{H NMR}$  ( $\text{DMSO}-d_6$ )  $\delta$  2.17 (s, 3H), 2.39 (s, 4H), 7.38–7.44 (m, 1H), 7.68 (s, 1H), 7.69–7.74 (m, 1H), 7.83 (d, 1H,  $J = 8.2$ ), 8.49–8.55 (m, 2H), 8.62 (s, 1H), 9.07 (s, 1H), 9.45 (d, 1H,  $J = 8.2$ ), 9.57 (s, 1H), 12.05 (s, 1H); HRMS calculated for  $\text{C}_{25}\text{H}_{19}\text{N}_6\text{O}_4$  ( $\text{M} + \text{H}^+$ ) 467.1468, found 467.1480.

**7-Amino-6-chloro-2-formylquinoline-5,8-dione (46).** In a dry 100 mL round-bottomed two-necked flask, equipped with a magnetic bar and water-cooled reflux condenser under argon, 7-amino-6-chloro-2-methylquinoline-5,8-dione<sup>44</sup> (**30**, 133.8 mg, 0.6 mmol), selenium dioxide (106.6 mg), 20 mL of dried and distilled 1,4-dioxane, and 0.09 mL of water were stirred at reflux in an oil bath for 23 h. The reaction was monitored by TLC. The mixture was hot filtered, and the solid was washed with hot chloroform. The filtrate was rotaevaporated to dryness. The dried material was dissolved in 480 mL of chloroform and washed with saturated sodium chloride solution (4 × 60 mL). The solution was dried over magnesium sulfate and rotaevaporated to dryness and then further dried under a vacuum pump. The product weighed 105.2 mg (74%): mp 220 °C (dec);  $^1\text{H NMR}$  ( $\text{CDCl}_3$ )  $\delta$  5.6 (br s, 2H), 8.28 (d, 1H,  $J =$

8.1), 8.67 (d, 1H,  $J = 8.1$ ), 10.30 (s, 1H); HRMS calculated for  $\text{C}_{10}\text{H}_6\text{ClN}_2\text{O}_3$  ( $\text{M} + \text{H}^+$ ) 237.0061, found 237.0068.

**6-Chlorolavendamyacin Methyl Ester (32).** In a setup similar to that used for the synthesis of **16**, 7-amino-6-chloro-2-formylquinoline-5,8-dione (**31**, 118.5 mg, 0.5 mmol) was placed with  $\beta$ -methyltryptophan methyl ester<sup>43</sup> (115 mg, 0.5 mmol) in 300 mL of dry anisole. The solution was stirred and heated slowly to 130 °C over 3 h. The reaction mixture was refluxed for 1 h. The mixture was then cooled to room temperature under argon. The solvent was rotaevaporated to dryness, and then the solid was washed with acetone (20 mL). The resulting solid was vacuum filtered and dried under a vacuum pump. The product weighed 131.9 mg (59%): mp > 270 °C,  $R_f = 0.09$  ( $\text{CHCl}_3$ , twice developed);  $^1\text{H NMR}$  ( $\text{CDCl}_3$ )  $\delta$  3.22 (s, 3H), 4.08 (s, 3H), 5.70 (br s, 2H), 7.38–7.45 (m, 1H), 7.65–7.71 (m, 1H), 7.80 (d, 1H,  $J = 8.0$ ), 8.38 (d, 1H,  $J = 7.7$ ), 8.61 (d, 1H,  $J = 8.4$ ), 9.10 (d, 1H,  $J = 8.4$ ), 11.89 (br s, 1H), CIMS  $m/e$  (relative intensity) 446.1 ( $\text{M}^+$ , 100), 416.0 (10.3), 386.0 (64.4), 351.1 (22.0), 113.0 (9.0); HRMS calculated for  $\text{C}_{23}\text{H}_{15}\text{N}_4\text{O}_4\text{Cl}$  446.0849, found 446.0781.

**5,7-Dibromo-8-hydroxy-2-methylquinoline (55).** The procedure for the preparation of **55** was similar to that of **56**, except that after the evaporation of the combined filtrates the dry residue was dissolved in 100 mL of chloroform, filtered, and then concentrated to small volume. The solution was kept in the refrigerator for a day to give a yellow product (455 mg, 29%): mp 234–235 °C;  $^1\text{H NMR}$  ( $\text{DMSO}-d_6$ )  $\delta$  8.14 (d, 1H,  $J = 8.8$ ), 8.25 (s, 1H), 8.63 (d, 1H,  $J = 8.8$ ), 10.19 (s, 1H), 11.31 (br s, 1H); HRMS calculated for  $\text{C}_{10}\text{H}_5\text{Br}_2\text{NO}_2$  328.8667, found 328.8667.

**3-Carbomethoxy-1-(5,7-Dibromo-8-hydroxyquinoline-2-yl)-4-methyl- $\beta$ -carboline (57).** In a setup similar to that used for **16**, 5,7-dibromo-2-formyl-8-hydroxyquinoline (165.5 mg, 0.5 mmol) and  $\beta$ -methyltryptophan methyl ester (115.5 mg, 0.5 mmol) in 70 mL of dry anisole were mixed. Heat was introduced, and the temperature was raised to reflux over a 3-h period and then refluxed for 39 more h. The reaction mixture was evaporated under reduced pressure, and the solid was dried under vacuum. The crude yellow solid weighed 217 mg, (80%). An analytical sample was obtained as follows: The material was stirred in a small volume of dichloromethane giving an orange solid. The filtrate was allowed to stand at room temperature to produce more of the pure **57**: mp 248 °C (dec);  $R_f = 0.62$  (0.3/5 pet. ether/EtOAc);  $^1\text{H NMR}$  ( $\text{CDCl}_3$ )  $\delta$  3.13 (s, 3H), 3.99 (s, 3H), 7.43 (dd, 1H,  $J = 8.1, 7.0$ ), 7.72 (dd, 1H,  $J = 8.1, 7.0$ ), 7.91 (d, 1H,  $J = 8.1$ ), 8.17 (s, 1H), 8.44 (d, 1H,  $J = 8.1$ ), 8.68 (d, 1H,  $J = 8.8$ ), 8.95 (d, 1H,  $J = 8.8$ ), 12.23 (br s, 1H); HRMS calculated for  $\text{C}_{23}\text{H}_{15}\text{Br}_2\text{N}_3\text{O}_3$  540.9454, found 540.9459.

**7-Bromodeaminolavendamyacin Methyl Ester (34).** In a 500 mL round-bottomed flask equipped with a condenser, a dropping funnel, a magnetic bar, and an argon-filled balloon, a mixture of 63.5 mg (0.117 mmol) of the crude **57** in 200 mL of acetonitrile–water (2/1, v/v) was dropwise added to a cold solution of 110.7 mg (0.257 mmol) of bis(trifluoroacetoxy)-iodobenzene in 33 mL of acetone–water (2/1, V/V) at 0 °C over 2 h and 40 min. The reaction mixture was stirred at this temperature for 6 more h. The mixture was evaporated under reduced pressure to remove acetonitrile and then extracted with chloroform (3 × 40 mL). The combined extracts were dried ( $\text{MgSO}_4$ ) and evaporated to give an impure orange product. Flash chromatography ( $\text{CHCl}_3/\text{EtOAc}$  250/3) gave 25.75 mg (46%) of the orange product **34**: mp 209 °C (dec);  $R_f = 0.62$  (0.4/5 EtOAc/ $\text{CH}_2\text{Cl}_2$ );  $^1\text{H NMR}$  ( $\text{CDCl}_3$ )  $\delta$  3.21 (s, 3H), 4.08 (s, 3H), 7.35–7.45 (m, 1H), 7.60 (s, 1H), 7.65–7.7 (m, 1H), 7.81 (d, 1H,  $J = 8.0$ ), 8.35 (d, 1H,  $J = 8.0$ ), 8.50 (d, 1H,  $J = 8.2$ ), 9.09 (d, 1H,  $J = 8.4$ ), 11.90 (br s, 1H); HRMS calculated for  $\text{C}_{23}\text{H}_{14}\text{BrN}_3\text{O}_4$  475.0162, found 475.0143.

**Decarboxy-2'-(hydroxymethyl)-demethyllavendamyacin (37).** In a dry 5 mL round-bottomed flask equipped with a condenser, a magnetic bar, and an argon-filled balloon, a mixture of acetamido compound **22** (24 mg, 0.0582 mmol) in 1 mL of 70% sulfuric acid solution ( $\text{H}_2\text{SO}_4/\text{H}_2\text{O}$  70/30, v/v) was heated in an oil bath at 60 °C for 2 h. The reaction mixture

was treated with a saturated solution of sodium carbonate to pH of 9 and then extracted with EtOAc ( $5 \times 20$  mL). The combined organic layers were washed with brine ( $2 \times 10$  mL), dried ( $\text{MgSO}_4$ ), and evaporated under reduced pressure to give 19 mg (88%) of a red solid: mp 255–260 °C (dec);  $R_f = 0.59$  (0.4/5 MeOH/ $\text{CH}_2\text{Cl}_2$ );  $^1\text{H NMR}$  (DMSO- $d_6$ )  $\delta$  4.85 (d, 2H), 5.54 (br s, 1H), 5.93 (br s, 2H), 7.33 (dd, 1H,  $J = 7.2$ ), 7.64 (dd, 1H,  $J = 7.2$ ), 7.69 (d, 1H,  $J = 8.0$ ), 8.36–8.38 (m, 2H), 8.46 (d, 1H,  $J = 8.0$ ), 8.88 (d, 1H,  $J = 8.0$ ), 11.64 (br s, 1H); HRMS calculated for  $\text{C}_{21}\text{H}_{14}\text{N}_4\text{O}_3$  370.1066, found 370.1072.

**Decarboxydemethylavendamyacin (38).** In a method similar to that of **37**, 20 mg (0.052 mmol) of compound **14** in 2.4 mL of 70%  $\text{H}_2\text{SO}_4$  was heated at 60 °C for 4 h to give **38** as a red solid (15 mg, 85%): mp > 270 °C;  $R_f = 0.47$  (0.2/5 MeOH/ $\text{CH}_2\text{Cl}_2$ );  $^1\text{H NMR}$  (DMSO- $d_6$ )  $\delta$  5.94 (br s, 2H), 7.3–7.4 (m, 1H), 7.65–7.8 (m, 2H), 8.36–8.38 (m, 2H), 8.48 (d, 1H,  $J = 8.0$ ), 8.59 (d, 1H,  $J = 8.4$ ), 8.91 (d, 1H,  $J = 8.4$ ), 11.77 (br s, 1H); HRMS calculated for  $\text{C}_{20}\text{H}_{12}\text{N}_4\text{O}_2$  340.0960, found 340.0597.

**2-Formyl-8-hydroxyquinoline (56).** In a 500 mL round-bottomed flask equipped with a magnetic bar, an argon-filled balloon, and a water-cooled condenser, 8-hydroxy-2-methylquinoline (**54**, 2 g, 12.4 mmol), selenium dioxide (1.74 g, 15.8 mmol), 300 mL of dried and distilled 1,4-dioxane, and 1.5 mL of water were mixed. The reaction mixture was heated, and the temperature was raised to reflux over a 2.5 h period. The mixture was refluxed for 21.5 h when thin-layer chromatography showed the completion of the reaction. The reaction mixture was filtered off, and the selenium metal was washed with 160 mL of dichloromethane. The combined filtrates were evaporated under reduced pressure to dryness. The residue was sublimed (at 81 °C, 0.15 mm/Hg) to give a pure yellow solid (1.337 g, 61%): mp 95–96 °C;  $^1\text{H NMR}$  ( $\text{CDCl}_3$ )  $\delta$  7.27 (d, 1H,  $J = 7.9$ ), 7.42 (d, 1H,  $J = 8.3$ ), 7.62 (t, 1H,  $J = 7.8$ ), 8.03 (s, 1H), 8.1 (d, 1H,  $J = 12.7$ ), 8.31 (d, 1H,  $J = 8.2$ ), 10.21 (s, 1H); MS  $m/z$  174 ( $\text{M}+\text{H}$ ) $^+$ , 173 and 172; Analysis for  $\text{C}_{10}\text{H}_7\text{NO}_2$  calculated C, 69.36; H, 4.07; N, 8.09, found C, 69.34; H, 4.2; N, 8.06.

**1-(8-Hydroxyquinoline-2-yl)- $\beta$ -carboline (58).** In a 100 mL three-necked round-bottomed flask equipped with a condenser, a magnetic bar, and flowing argon, 2-formyl-8-hydroxyquinoline (**56**, 35.5 mg, 0.2 mmol), tryptamine (32.6 mg, 0.2 mmol) and 20 mL of dried distilled anisole were mixed together. The mixture was heated, and the temperature was raised to reflux over the course of 4 h and then refluxed for 22 h. To the mixture was added 10 mg of 5% Pd/C, and after 7 more hours of reflux another 5 mg of Pd/C was added and then refluxed for 20 more hours. The mixture was filtered and rotaevaporated to dryness. The material was recrystallized from acetone giving 48 mg (76%) of a yellow solid: mp 276–279 °C;  $R_f = 0.12$  (0.4/5 MeOH/ $\text{CH}_2\text{Cl}_2$ );  $^1\text{H NMR}$  (DMSO- $d_6$ )  $\delta$  7.28 (m, 1H), 7.34 (dd, 1H,  $J = 7.6$ ), 7.52 (d, 1H,  $J = 5.0$ ), 7.65 (dd, 1H,  $J = 8.0$ , 7.8), 7.77 (d, 1H,  $J = 8.0$ ), 8.32 (d, 1H,  $J = 5.0$ ), 8.36 (d, 1H,  $J = 8.0$ ), 8.51 (d, 1H,  $J = 8.8$ ), 8.59 (d, 1H,  $J = 5.0$ ), 8.82 (d, 1H,  $J = 8.8$ ), 10.35 (s, 1H), 12.16 (br s, 1H); HRMS calculated for  $\text{C}_{20}\text{H}_{13}\text{N}_3\text{O}$  311.1058, found 311.1045.

**Deaminodecarboxydemethylavendamyacin (39).** Compound **39** was obtained in a procedure similar to that of **34** except that the reaction was performed in a 250 mL flask. A solution of 3-carbomethoxy-1-(8-hydroxyquinoline-2-yl)- $\beta$ -carboline (**58**, 15 mg, 0.048 mmol) in 120 mL of acetonitrile–water (2/1, v/v) was dropwise added to a solution of bis(trifluoroacetoxy)iodobenzene (41.5 mg, 0.096 mmol) in 7.5 mL of acetonitrile–water at 0 °C over a 2 h period. The mixture was allowed to stir at this temperature for another 2 h and then evaporated in vacua to remove acetonitrile. The residue was extracted with dichloromethane ( $3 \times 25$  mL), dried ( $\text{MgSO}_4$ ), and evaporated to give 12 mg (77%) of the orange product **39**: mp 227–229 °C (dec);  $R_f = 0.33$  (0.003/5 MeOH/ $\text{CH}_2\text{Cl}_2$ );  $^1\text{H NMR}$  ( $\text{CDCl}_3$ )  $\delta$  7.07 (dd, 1H,  $J = 10.4$ ), 7.16 (dd, 1H,  $J = 10.4$ ), 7.31 (dd, 1H,  $J = 7.2$ ), 7.62 (dd, 1H,  $J = 7.2$ ), 7.75 (d, 1H,  $J = 8.0$ ), 8.10 (d, 1H,  $J = 5.0$ ), 8.17 (d, 1H,  $J = 7.8$ ), 8.50 (d, 1H,  $J = 8.4$ ), 8.58 (d, 1H,  $J = 5.0$ ), 9.02 (d, 1H,  $J = 8.4$ ), 11.69 (br s, 1H); HRMS calculated for  $\text{C}_{20}\text{H}_{11}\text{N}_3\text{O}_2$  325.0851, found 325.0862.

**Electrochemistry.** Cyclic voltammetry (CV) for 14 lavendamyacin analogues was conducted using a BAS CV-50W electrochemical analyzer equipped with a standard three-electrode cell. This cell was designed to allow the tip of the reference electrode to approach closely to the working electrode. Voltammetric experiments were performed using Ag/AgCl as the reference electrode, a glossy carbon (GC) rod as the working electrode, and a platinum (Pt) wire as the auxiliary electrode. Potential data are referred to the Ferrocene (0/+ ) couple, which is oxidized in DMSO at +0.52 V vs Ag/AgCl. Positive-feedback  $iR$  compensation was routinely applied. The working electrode was regularly polished using alumina. Typically, a solution containing 1 mM of the lavendamyacin analogues and 0.1 M supporting electrolyte (tetrabutylammonium hexafluorophosphate,  $\text{Bu}_4\text{NPF}_6$ ) was prepared using dried dimethyl sulfoxide (DMSO). All samples were purged with argon prior to use and kept under a continuous flow of argon during the course of the experiments. All CV data were recorded at a potential range between 0.00 and –2.00 V and at potential sweep rates of 50 to 500 mV/s. All measurements were performed at  $22 \pm 1$  °C.

**Biological Studies. Cell Culture.** BE-WT and BE-NQ cells were a gift from Dr. David Ross (University of Colorado Health Sciences Center, Denver, CO). Cells were grown in minimum essential medium (MEM) with Earle's salts, nonessential amino acids, L-glutamine and penicillin/streptomycin and supplemented with 10% fetal bovine serum (FBS), sodium bicarbonate and HEPES. Cell culture medium and supplements were obtained from Gibco, Invitrogen Co., Grand Island, NY. The cells were incubated at 37 °C under a humidified atmosphere containing 5%  $\text{CO}_2$ .

**Cytochrome *c* Assay.** Lavendamyacin analogues reduction was monitored using a spectrophotometric assay in which the rate of reduction of cytochrome *c* was quantified at 550 nm. Briefly, the assay mixture contained cytochrome *c* (70  $\mu\text{M}$ ), NADH (1 mM), human recombinant NQO1 (0.1–3  $\mu\text{g}$ ) (gift from Dr. David Ross, University of Colorado Health Sciences Center, Denver, CO), and lavendamyacin (25  $\mu\text{M}$ ) in a final volume of 1 mL of Tris-HCl (25 mM, pH 7.4) containing 0.7 mg/mL BSA and 0.1% Tween-20. Reactions were carried out at room temperature and started by the addition of NADH. Rates of reduction were calculated from the initial linear part of the reaction curve (0–30 s), and results were expressed in terms of  $\mu\text{mol}$  of cytochrome *c* reduced/min/mg of NQO1 using a molar extinction coefficient of  $21.1 \text{ mM}^{-1} \text{ cm}^{-1}$  for cytochrome *c*. All reactions were carried out in triplicate.

**MTT Assay.** Growth inhibition was determined using the MTT colorimetric assay. Cells were plated in 96-well plates at a density of 10000 cells/mL and allowed to attach overnight (16 h). Lavendamyacin analogues solutions were applied in medium for 2 h. Lavendamyacin analogues solutions were removed and replaced with fresh medium and 96-well plates were incubated at 37 °C under a humidified atmosphere containing 5%  $\text{CO}_2$  for 4–5 days. MTT (50  $\mu\text{g}$ ) was added, and the cells were incubated for another 4 h. Medium/MTT solutions were removed carefully by aspiration, the MTT formazan crystals were dissolved in 100  $\mu\text{L}$  of DMSO, and absorbance was determined on a plate reader at 560 nm.  $\text{IC}_{50}$  values (concentration at which cell survival equals 50% of control) were determined from semilog plots of percent of control vs concentration. Selectivity ratios were defined as the  $\text{IC}_{50}$  value for the BE-WT cell line divided by the  $\text{IC}_{50}$  value for the BE-NQ cell line.

**Clonogenic Assay.** Cells were harvested from logarithmic-phase growing cultures and plated at densities of 1000 cells per 100-mm dish to yield a readily quantifiable number of colonies at the end of the experiment. After 24 h, cells were treated with lavendamyacin analogues, 2% DMSO (drug vehicle), or no treatment (control) for 2 h at 37 °C. After 2 h, drug-containing medium was replaced with fresh drug-free medium. Cells were incubated at 37 °C under a humidified atmosphere containing 5%  $\text{CO}_2$  for 12 days. Then, the medium was removed, and colonies were washed twice with PBS, fixed and stained with 0.1% (w/v) Coomassie Blue dye in 30%



methanol and 10% acetic acid for 1–2 min. Surviving colonies (>50 cells) were counted and the surviving fraction determined by dividing the number of colonies in a treatment dish by the number of colonies in the control dish. IC<sub>50</sub> values (concentration at which cell survival equals 50% of control) were determined from semilog plots of percent of control vs concentration. Selectivity ratios were defined as the IC<sub>50</sub> value for the BE-WT cell line divided by the IC<sub>50</sub> value for the BE-NQ cell line.

**Molecular Modeling. Coordinates Preparation.** The coordinates of the crystal structure of human NQO1 complex with bound FAD and **65**, obtained from the Protein Data Bank (PDB ID code: 1H69<sup>25</sup>), were used as a reference structure for the docking experiments, and compound **65** served as the original reference ligand. The physiological dimer in the crystal unit was used for docking purposes. The coordinates were locally minimized. The coordinates were subjected to energy minimization with minimal iterations (100) by Powell minimization standard method using Minimize Subset option. This option automatically selected 24 seed amino acid residues surrounding the superposed ligand **37** (refer to the Docking section below) to perform the local minimization. Default parameters and values within the minimization dialogue were used except where otherwise mentioned. This procedure yielded a weighted root-mean-square distance of 0.26 Å between the 24 corresponding nonminimized and minimized residues in the structures. Docking calculations were performed using one of the two identical active sites.

**Ligand Preparation.** The structures of ligands were sketched and prepared as MOL2 files employing the Sketch Molecule module of SYBYL 6.9.1 software suite<sup>58</sup> (Tripos, Inc.; St. Louis, MO). Initially sketched ligands were subjected to energy minimization (10000 iterations) by Powell minimization standard method. Initial Optimization and Termination parameters were set to None and Energy Change options, respectively. Default parameters and values within the minimization dialogue (Minimize Details) were used except where otherwise mentioned. The final ligand conformational coordinates were stored as MOL2 files within the database.

**Docking.** Flexible docking was performed using the FlexX module of SYBYL 6.9.1 software suite.<sup>58</sup> FlexX is an automatic docking program for conformationally flexible ligands, employs the three-dimensional structure of the target protein in PDB format, and is capable of determining 30 possible conformations for each docked ligand. The final ranking order of conformations is based on the free binding energy. This program automatically selects the base fragment of a ligand (the ligand core). The base fragment is then placed into the active site of the target protein using the algorithmic approach called pose clustering that is based upon a pattern recognition paradigm. Subsequent incremental reconstruction of the complete ligand molecule is then performed by linking the remaining components.<sup>59,60</sup> In this study, to define the active site, the energy-minimized ligand **37** was superpositioned to the coordinates of the original reference ligand **65** such that overlap was optimal. Ligand **37** was again energy minimized in the context of the active site, and therefore the position of the ligand within the pocket was optimized. The active site was then defined as all the amino acid residues confined within 6.5 Å radius sphere centered on the superposed ligand **37**. FAD was introduced to the active site as a heteroatom file in MOL2 format.

**Scoring Functions.** The docked conformations of ligands were evaluated and ranked using FlexX and four scoring functions implemented in the CSCORE module in SYBYL. CSCORE is a consensus scoring program that integrates multiple well-known scoring functions such as FlexX and ChemScore,<sup>61</sup> D-Score,<sup>62</sup> G-Score,<sup>63</sup> and PMF-Score<sup>64</sup> to evaluate docked conformations. Individual scoring functions are used to predict the affinity of the ligand binding to a target protein. CSCORE creates columns in a molecular spreadsheet that contain raw scores for each individual scoring function. The consensus column contains integers that range from 0 to 5; where 5 is the best fit to the model. Docked conformations

whose scores exceed the threshold for a particular function contribute one to the value of the consensus, whereas those with scores below the threshold add a zero.

**Molecular Graphics System.** The molecular graphics images and surface representations were prepared by PyMOL molecular graphics system version PyMOLX11Hybrid 0.97<sup>66</sup> (Delano Scientific, San Carlos, CA). The data of the coordinates of the NQO1 complex with bound FAD and docked conformations of ligands were prepared in PDB format as PyMOL input files. PyMOL session files of the NQO1 active site with docked conformations of ligands and the superimposition of clustered conformations were created. The images were then stored as graphic files.

**Acknowledgment.** We acknowledge financial support from the American Cancer Society and the National Institutes of Health (NIH grants: R15 CA78232, H.D.B.; NCRP P20 RR15583, J.M.G.; and CA74245, M.B.). We thank Professor David Williams, his graduate student Andrew Donnell, and the staff at the Mass Spectroscopy Laboratory of Indiana University for their assistance in obtaining mass spectral data. We also thank Professor Edward Rosenberg and his graduate student Dalia Rokhsana at the Department of Chemistry of the University of Montana for their assistance with the electrochemistry. The expert assistance of Rohn Wood in the Molecular Computational Core Facility of the University of Montana is greatly appreciated.

**Supporting Information Available:** NMR spectra for compounds **4**, **14–25**, **32**, **34**, **37–39**, **41**, and **46**, analytical data for compounds **14–25**, **32**, **34**, **37–39**, and geometric post-docking analyses of the poses of compounds **31** and **37** are available free of charge via the Internet at <http://pubs.acs.org>.

## References

- (1) Workman, P. Keynote address: Bioreductive mechanisms. *Int. J. Radiat. Oncol. Biol. Phys.* **1992**, *22*, 631–637.
- (2) Rooseboom, M.; Commandeur, J. N.; Vermeulen, N. P. Enzyme-catalyzed activation of anticancer prodrugs. *Pharmacol. Rev.* **2004**, *56*, 53–102.
- (3) Beall, H. D.; Winski, S. I. Mechanisms of action of quinone-containing alkylating agents. I: NQO1-directed drug development. *Front. Biosci.* **2000**, *5*, 639–648.
- (4) Phillips, R. M. Prospects for bioreductive drug development. *Exp. Opin. Invest. Drugs* **1998**, *7*, 905–928.
- (5) Workman, P. Enzyme-directed bioreductive drug development revisited: A commentary on recent progress and future prospects with emphasis on quinone anticancer agents and quinone metabolizing enzymes, particularly DT-diaphorase. *Oncol. Res.* **1994**, *6*, 461–475.
- (6) Skelly, J. V.; Sanderson, M. R.; Suter, D. A.; Baumann, U.; Read, M. A.; Gregory, D. S.; Bennett, M.; Hobbs, S. M.; Neidle, S. Crystal structure of human DT-diaphorase: A model for interaction with the cytotoxic prodrug 5-(aziridin-1-yl)-2,4-dinitrobenzamide (CB1954). *J. Med. Chem.* **1999**, *42*, 4325–4330.
- (7) Danson, S.; Ward, T. H.; Butler, J.; Ranson, M. DT-diaphorase: A target for new anticancer drugs. *Cancer Treat. Rev.* **2004**, *30*, 437–449.
- (8) Lind, C.; Cadenas, E.; Hochstein, P.; Ernster, L. DT-diaphorase: Purification, properties, and function. *Methods Enzymol.* **1990**, *186*, 287–301.
- (9) Faig, M.; Bianchet, M. A.; Talalay, P.; Chen, S.; Winski, S.; Ross, D.; Amzel, L. M. Structures of recombinant human and mouse NAD(P)H: quinone oxidoreductases: Species comparison and structural changes with substrate binding and release. *Proc. Natl. Acad. Sci. U.S.A.* **2000**, *97*, 3177–3182.
- (10) Li, R.; Bianchet, M. A.; Talalay, P.; Amzel, L. M. The three-dimensional structure of NAD(P)H: quinone reductase, a flavoprotein involved in cancer chemoprotection and chemotherapy: Mechanism of the two-electron reduction. *Proc. Natl. Acad. Sci. U.S.A.* **1995**, *92*, 8846–8850.
- (11) Eliasson, M.; Bostrom, M.; DePierre, J. W. Levels and subcellular distributions of detoxifying enzymes in the ovarian corpus luteum of the pregnant and non-pregnant pig. *Biochem. Pharmacol.* **1999**, *58*, 1287–1292.
- (12) Winski, S. L.; Koutalos, Y.; Bentley, D. L.; Ross, D. Subcellular localization of NAD(P)H:quinone oxidoreductase 1 in human cancer cells. *Cancer Res.* **2002**, *62*, 1420–1424.

- (13) Ernster, L. DT Diaphorase. *Methods Enzymol.* **1967**, *10*, 309–317.
- (14) Ernster, L. DT Diaphorase: A historical review. *Chem. Scripta* **1987**, *27A*, 1–13.
- (15) Siegel, D.; Gibson, N. W.; Preusch, P. C.; Ross, D. Metabolism of mitomycin C by DT-diaphorase: Role in mitomycin C-induced DNA damage and cytotoxicity in human colon carcinoma cells. *Cancer Res.* **1990**, *50*, 7483–7489.
- (16) Walton, M. I.; Smith, P. J.; Workman, P. The role of NAD(P)H: quinone reductase (EC 1.6.99.2, DT-diaphorase) in the reductive bioactivation of the novel indolequinone antitumor agent EO9. *Cancer Commun.* **1991**, *3*, 199–206.
- (17) Siegel, D.; Beall, H. D.; Senekowitsch, C.; Kasai, M.; Arai, H.; Gibson, N. W.; Ross, D. Bioreductive activation of mitomycin C by DT-diaphorase. *Biochemistry* **1992**, *31*, 7879–7885.
- (18) Naylor, M. A.; Swann, E.; Everett, S. A.; Jaffar, M.; Nolan, J.; Robertson, N.; Lockyer, S. D.; Patel, K. B.; Dennis, M. F.; Stratford, M. R.; Wardman, P.; Adams, G. E.; Moody, C. J.; Stratford, I. J. Indolequinone antitumor agents: Reductive activation and elimination from (5-methoxy-1-methyl-4,7-dioxindol-3-yl)methyl derivatives and hypoxia-selective cytotoxicity in vitro. *J. Med. Chem.* **1998**, *41*, 2720–2731.
- (19) Siegel, D.; Gibson, N. W.; Preusch, P. C.; Ross, D. Metabolism of diaziquone by NAD(P)H:(quinone acceptor) oxidoreductase (DT-diaphorase): Role in diaziquone-induced DNA damage and cytotoxicity in human colon carcinoma cells. *Cancer Res.* **1990**, *50*, 7293–7300.
- (20) Schlager, J. J.; Powis, G. Cytosolic NAD(P)H:(quinone-acceptor)-oxidoreductase in human normal and tumor tissue: Effects of cigarette smoking and alcohol. *Int. J. Cancer* **1990**, *45*, 403–409.
- (21) Malkinson, A. M.; Siegel, D.; Forrest, G. L.; Gazdar, A. F.; Oie, H. K.; Chan, D. C.; Bunn, P. A.; Mabry, M.; Dykes, D. J.; Harrison, S. D.; Ross, D. Elevated DT-diaphorase activity and messenger RNA content in human non small cell lung carcinoma: Relationship to the response of lung tumor xenografts to mitomycin C. *Cancer Res.* **1992**, *52*, 4752–4757.
- (22) Cresteil, T.; Jaiswal, A. K. High levels of expression of the NAD-(P)H: quinone oxidoreductase (NQO1) gene in tumor cells compared to normal cells of the same origin. *Biochem. Pharmacol.* **1991**, *42*, 1021–1027.
- (23) Rampling, R.; Cruickshank, G.; Lewis, A. D.; Fitzsimmons, S. A.; Workman, P. Direct measurement of pO<sub>2</sub> distribution and bioreductive enzymes in human malignant brain tumors. *Int. J. Radiat. Oncol. Biol. Phys.* **1994**, *29*, 427–431.
- (24) Mikami, K.; Naito, M.; Ishiguro, T.; Yano, H.; Tomida, A.; Yamada, T.; Tanaka, N.; Shirakusa, T.; Tsuruo, T. Immunological quantitation of DT-diaphorase in carcinoma cell lines and clinical colon cancers: Advanced tumors express greater levels of DT-diaphorase. *Jpn. J. Cancer Res.* **1998**, *89*, 910–915.
- (25) Faig, M.; Bianchet, M. A.; Winski, S.; Hargreaves, R.; Moody, C. J.; Hudnott, A. R.; Ross, D.; Amzel, L. M. Structure-based development of anticancer drugs: Complexes of NAD(P)H: quinone oxidoreductase 1 with chemotherapeutic quinones. *Structure* **2001**, *9*, 659–667.
- (26) Winski, S. L.; Faig, M.; Bianchet, M. A.; Siegel, D.; Swann, E.; Fung, K.; Duncan, M. W.; Moody, C. J.; Amzel, L. M.; Ross, D. Characterization of a mechanism-based inhibitor of NAD(P)H: quinone oxidoreductase 1 by biochemical, X-ray crystallographic, and mass spectrometric approaches. *Biochemistry* **2001**, *40*, 15135–15142.
- (27) Zhou, Z.; Fisher, D.; Spidel, J.; Greenfield, J.; Patson, B.; Fazal, A.; Wigal, C.; Moe, O. A.; Madura, J. D. Kinetic and docking studies of the interaction of quinones with the quinone reductase active site. *Biochemistry* **2003**, *42*, 1985–1994.
- (28) Cavelier, G.; Amzel, L. M. Mechanism of NAD(P)H: quinone reductase: Ab initio studies of reduced flavin. *Proteins: Struct. Funct. Genet.* **2001**, *43*, 420–432.
- (29) Doyle, T. W.; Balitz, D. M.; Grulich, R. E.; Nettleton, D. E.; Gould, S. J.; Tann, C.; Moews, A. E. Structure determination of lavendamycin, a new antitumor antibiotic from *Streptomyces lavendulae*. *Tetrahedron Lett.* **1981**, *22*, 4595–4598.
- (30) Balitz, D. M.; Bush, J. A.; Bradner, W. T.; Doyle, T. W.; O'Herron, F. A.; Nettleton, D. E. Isolation of lavendamycin, a new antibiotic from *Streptomyces lavendulae*. *J. Antibiot. (Tokyo)* **1982**, *35*, 259–265.
- (31) Erickson, W. R.; Gould, S. J. Streptonigrin biosynthesis. 7. Incorporation of oxygen from <sup>18</sup>O<sub>2</sub>: Evidence for an oxidative β-carboline cleavage. *J. Am. Chem. Soc.* **1985**, *107*, 5831–5832.
- (32) Erickson, W. R.; Gould, S. J. Streptonigrin Biosynthesis. 8. Evidence for the involvement of a new Shikimate pathway product and a new route to quinolines. *J. Am. Chem. Soc.* **1987**, *109*, 620–621.
- (33) Rao, K. V.; Biemann, K.; Woodward, R. B. The structure of streptonigrin. *J. Am. Chem. Soc.* **1963**, *85*, 2532–2533.
- (34) Boger, D. L.; Yasuda, M.; Mitscher, L. A.; Drake, S. D.; Kitos, P. A.; Thompson, S. C. Streptonigrin and lavendamycin partial structures. Probes for the minimum, potent pharmacophore of streptonigrin, lavendamycin, and synthetic quinoline-5,8-diones. *J. Med. Chem.* **1987**, *30*, 1918–1928.
- (35) Hackethal, C. A.; Golbey, R. B.; Tan, C. T.; Karnofsky, D. A.; Burchenal, J. H. Clinical observations on the effects of streptonigrin in patients with neoplastic disease. *Antibiot. Chemother.* **1961**, *11*, 178–183.
- (36) Fang, Y.; Linardic, C. M.; Richardson, D. A.; Cai, W.; Behforouz, M.; Abraham, R. T. Characterization of the cytotoxic activities of novel analogues of the antitumor agent, lavendamycin. *Mol. Cancer Ther.* **2003**, *2*, 517–526.
- (37) Behforouz, M.; Merriman, R. L. Lavendamycin analogues and methods of making and using them. U.S. Patent 5525611, 1996.
- (38) Behforouz, M.; Cai, W.; Stocksdale, M. G.; Lucas, J. S.; Jung, J. Y.; Briere, D.; Wang, A.; Katzen, K. S.; Behforouz, N. C. Novel lavendamycin analogues as potent HIV-reverse transcriptase inhibitors: Synthesis and evaluation of anti-reverse transcriptase activity of amide and ester analogues of lavendamycin. *J. Med. Chem.* **2003**, *46*, 5773–5780.
- (39) Kende, A. S.; Ebetino, F. H. The regioselective total synthesis of lavendamycin methyl ester. *Tetrahedron Lett.* **1984**, *25*, 923–926.
- (40) Boger, D. L.; Duff, S. R.; Panek, J. S.; Yasuda, M. Total synthesis of lavendamycin methyl ester. *J. Org. Chem.* **1985**, *50*, 5790–5795.
- (41) Behforouz, M.; Gu, Z.; Cai, W.; Horn, M. A.; Ahmadian, M. A highly concise synthesis of lavendamycin methyl ester. *J. Org. Chem.* **1993**, *58*, 7089–7091.
- (42) Behforouz, M.; Haddad, J.; Cai, W.; Arnold, M. B.; Mohammadi, F.; Sousa, A. C.; Horn, M. A. Highly efficient and practical syntheses of lavendamycin methyl ester and related novel quinolindiones. *J. Org. Chem.* **1996**, *61*, 6552–6555.
- (43) Behforouz, M.; Zarrinmayeh, H.; Ogle, M. E.; Riehle, T. J.; Bell, F. W. β-Carbolines derived from β-methyltryptophan and a stereoselective synthesis of (2RS,3SR)-β-methyltryptophan methyl ester. *J. Heterocycl. Chem.* **1988**, *25*, 1627–1632.
- (44) Behforouz, M.; Haddad, J.; Cai, W.; Gu, Z. Chemistry of quinoline-5,8-diones. *J. Org. Chem.* **1998**, *63*, 343–346.
- (45) Seradj, H.; Cai, W.; Erasga, N. O.; Chenault, D. V.; Knuckles, K. A.; Ragains, J. R.; Behforouz, M. Total synthesis of novel 6-substituted lavendamycin antitumor agents. *Org. Lett.* **2004**, *6*, 473–476.
- (46) Barret, R.; Daudon, M. Oxidation of phenols to quinones by bis-(trifluoroacetoxy)iodobenzene. *Tetrahedron Lett.* **1990**, *31*, 4871–4872.
- (47) Tolstikov, V. V.; Holpne Kozlova, N. V.; Oreshkina, T. D.; Osipova, T. V.; Preobrazhenskaya, M. N.; Sztaricskai, F.; Balzarini, J.; De Clercq, E. Amides of antibiotic streptonigrin and amino dicarboxylic acids or aminosugars. Synthesis and biological evaluation. *J. Antibiot. (Tokyo)* **1992**, *45*, 1020–1025.
- (48) Cotterill, A. S.; Moody, C. J.; Mortimer, R. J.; Norton, C. L.; O'Sullivan, N.; Stephens, M. A.; Stradiotto, N. R.; Swann, E.; Stratford, I. J. Cyclopropamitosenes, novel bioreductive anticancer agents. Synthesis, electrochemistry, and biological activity of 7-substituted cyclopropamitosenes and related indolequinones. *J. Med. Chem.* **1994**, *37*, 3834–3843.
- (49) Beall, H. D.; Winski, S.; Swann, E.; Hudnott, A. R.; Cotterill, A. S.; O'Sullivan, N.; Green, S. J.; Bien, R.; Siegel, D.; Ross, D.; Moody, C. J. Indolequinone antitumor agents: Correlation between quinone structure, rate of metabolism by recombinant human NAD(P)H: quinone oxidoreductase, and in vitro cytotoxicity. *J. Med. Chem.* **1998**, *41*, 4755–4766.
- (50) Swann, E.; Barraja, P.; Oberlander, A. M.; Gardipee, W. T.; Hudnott, A. R.; Beall, H. D.; Moody, C. J. Indolequinone antitumor agents: Correlation between quinone structure and rate of metabolism by recombinant human NAD(P)H: quinone oxidoreductase. Part 2. *J. Med. Chem.* **2001**, *44*, 3311–3319.
- (51) Fryatt, T.; Pettersson, H. I.; Gardipee, W. T.; Bray, K. C.; Green, S. J.; Slawin, A. M.; Beall, H. D.; Moody, C. J. Novel quinoline-quinone antitumor agents: Structure-metabolism studies with NAD(P)H: quinone oxidoreductase (NQO1). *Bioorg. Med. Chem.* **2004**, *12*, 1667–1687.
- (52) Phillips, R. M.; Naylor, M. A.; Jaffar, M.; Doughty, S. W.; Everett, S. A.; Breen, A. G.; Choudry, G. A.; Stratford, I. J. Bioreductive activation of a series of indolequinones by human DT-diaphorase: Structure-activity relationships. *J. Med. Chem.* **1999**, *42*, 4071–4080.
- (53) Winski, S. L.; Hargreaves, R. H.; Butler, J.; Ross, D. A new screening system for NAD(P)H:quinone oxidoreductase (NQO1)-directed antitumor quinones: Identification of a new aziridinyl-hfbenzoquinone, RH1, as a NQO1-directed antitumor agent. *Clin. Cancer Res.* **1998**, *4*, 3083–3088.

- (54) Phillips, R. M.; Jaffar, M.; Maitland, D. J.; Loadman, P. M.; Shnyder, S. D.; Steans, G.; Cooper, P. A.; Race, A.; Patterson, A. V.; Stratford, I. J. Pharmacological and biological evaluation of a series of substituted 1,4-naphthoquinone bioreductive drugs. *Biochem. Pharmacol.* **2004**, *68*, 2107–2116.
- (55) Suleman, A.; Skibo, E. B. A comprehensive study of the active site residues of DT-diaphorase: Rational design of benzimidazole derivatives as DT-diaphorase substrates. *J. Med. Chem.* **2002**, *45*, 1211–1220.
- (56) Hendriks, H. R.; Pizao, P. E.; Berger, D. P.; Kooistra, K. L.; Bibby, M. C.; Boven, E.; Dreef-van der Meulen, H. C.; Henrar, R. E. C.; Fiebig, H. H.; Double, J. A.; Hornstra, H. W.; Pinedo, H. M.; Workman, P.; Schwartzmann, G. EO9: A novel bioreductive alkylating indoloquinone with preferential solid tumour activity and lack of bone marrow toxicity in preclinical models. *Eur. J. Cancer* **1993**, *29A*, 897–906.
- (57) Abe, N.; Nakakita, Y.; Nakamura, T.; Enoki, N.; Uchida, H.; Takeo, S.; Munekata, M. Novel cytotoxic compounds, oxopropalines from *Streptomyces* sp. G324 producing lavendamycin. I. Taxonomy of the producing organism, fermentation, isolation and biological activities. *J. Antibiot. (Tokyo)* **1993**, *46*, 1672–1677.
- (58) SYBYL molecular modeling software; SYBYL 6.9.1 ed.; Tripos Inc.: St. Louis, MO.
- (59) Lemmen, C.; Lengauer, T. Time-efficient flexible superposition of medium-sized molecules. *J. Comput.-Aided Mol. Des.* **1997**, *11*, 357–368.
- (60) Rarey, M.; Kramer, B.; Lengauer, T.; Klebe, G. A fast flexible docking method using an incremental construction algorithm. *J. Mol. Biol.* **1996**, *261*, 470–489.
- (61) Eldridge, M. D.; Murray, C. W.; Auton, T. R.; Paolini, G. V.; Mee, R. P. Empirical scoring functions: I. The development of a fast empirical scoring function to estimate the binding affinity of ligands in receptor complexes. *J. Comput.-Aided Mol. Des.* **1997**, *11*, 425–445.
- (62) Kuntz, I. D.; Blaney, J. M.; Oatley, S. J.; Langridge, R.; Ferrin, T. E. A geometric approach to macromolecule-ligand interactions. *J. Mol. Biol.* **1982**, *161*, 269–288.
- (63) Jones, G.; Willett, P.; Glen, R. C.; Leach, A. R.; Taylor, R. Development and validation of a genetic algorithm for flexible docking. *J. Mol. Biol.* **1997**, *267*, 727–748.
- (64) Muegge, I.; Martin, Y. C. A general and fast scoring function for protein–ligand interactions: A simplified potential approach. *J. Med. Chem.* **1999**, *42*, 791–804.
- (65) Allen, C. F. H.; Spangler, F. W.; Webster, E. R. Ethylenimine. *Org. Synth.* **1963**, *Coll. Vol. IV*, 433–435.
- (66) DeLano, W. L. *The PyMOL molecular graphics system*; PyMOLX11Hybrid ed.; DeLano Scientific: San Carlos, CA.

JM050758Z